ISSN 0037-8437

ANALES

DE LA

SOCIEDAD CIENTIFICA ARGENTINA

AÑO 2019 - VOLUMEN 265 - Nº 1

SUMARIO

Pág.

A.Alonso, A.B.Pomilio, S.R.Rodríguez, S.M.Battista, K.Mouchián, A.Vitale - "FUNGAL HYPERSENSITIVITY IN NASAL PATHOLOGIES". 5

Steve Chien, David Mclaren, Joshua Doubleday, Daniel Tran - USING HIGH-RESOLUTION, TASKABLE REMOTE SENSING IMAGERY TO SUPPORT A SENSORWEB FOR THAILAND FLOOD MONITORING 17

Dra. Daniela López De Luise - EL USO DE SOFT COMPUTING PARA EL MODELADODEL RAZONAMIENTO 39

ANALES

DE LA

SOCIEDAD CIENTIFICA ARGENTINA

AÑO 2019 - VOLUMEN 265 - Nº 1

Indizada en Biodiversity Heritage Library, Smithsonian Institute (USA),
en el Natural History Museum Library (UK) y en la
Ernst Mayr Library de Harvard University (USA).

Avda. SANTA FE 1145
C1059ABF BUENOS AIRES - ARGENTINA
Correo Electrónico: sociedad@cientifica.org.ar
www.cientifica.org.ar

EX PRESIDENTES DE LA SOCIEDAD CIENTIFICA ARGENTINA

1872-1874 Ing. Luis A. Huergo
1874-1875 Dr. Juan J. J. Kyle
1875-1877 Ing. Pedro Pico
1877-1878 Ing. Guillermo White
1878-1879 Ing. Luis A. Huergo
1879-1880 Dr. Valentín Balbín
1880-1881 Dr. Carlos Berg
1881-1882 Ing. Luis A. Huergo
1882-1883 Dr. Carlos Berg
1883-1885 Ing. Guillermo White
1885-1886 Ing. Luis A. Viglione
1886-1887 Dr. Estanislao S. Zeballos
1887-1889 Dr. Valentín Balbín
1889-1891 Dr. Carlos Maria Morales
1891-1892 Ing. Eduardo Aguirre
1892-1893 Dr. Juan J. J. Kyle
1893-1894 Ing. Carlos Bunge
1894-1895 Ing. Miguel Iturbe
1895-1896 Dr. Carlos Maria Morales
1896-1897 Dr. Angel Gallardo
1897-1898 Ing. Domingo Nocetti
1898-1900 Ing. Dr. Marcial R. Candiotti
1900-1901 Dr. Manuel B. Bahía
1901-1902 Dr. Carlos Maria Morales
1902-1903 Ing. Carlos Echagüe
1903-1904 Ing. Emilio Palacio
1904-1906 Dr. Carlos Maria Morales
1906-1908 Ing. Gral. Arturo M. Lugones
1908-1909 Ing. Otto Krause
1909-1910 Ing. Vicente Castro
1910-1911 Dr. Francisco P. Moreno
1911-1912 Ing. Vicente Castro
1912-1913 Gral. Dr. Agustín Alvarez
1913-1914 Ing. Santiago E. Barabino
1914-1915 Dr. Francisco P. Lavalle
1915-1917 Ing. Nicolás Besio Moreno
1917-1919 Dr. Carlos Maria Morales
1919-1923 Ing. Santiago E. Barabino
1923-1927 Ing. Eduardo Huergo
1927-1929 Ing. Nicolás Besio Moreno
1929-1933 Dr. Nicolás Lozano
1933-1937 Ing. Nicolás Besio Moreno
1937-1943 Ing. Jorge W. Dobranich
1943-1946 Dr. Gonzalo Bosch
1946-1949 Ing. José M. Páez
1949-1951 Ing. Dr. Eduardo María Huergo
1951-1956 Dr. Abel Sánchez Díaz
1956-1959 Dr. Eduardo Braun Menéndez
1959-1962 Ing. Pedro Longhini
1962-1964 Dr. Pablo Negroni
1964-1970 Ing. José S. Gandolfo
1970-1976 C. de Nav. Emilio L. Díaz
1976-1988 Ing. Agr. Eduardo Pous Peña
1988-1989 Ing. Augusto L. Bacqué
1989-1992 Ing. Lucio R. Ballester
1993-1999 Dr. Arturo Otaño Sahores
1999-2001 Dr. Andrés O. M. Stoppani
2001-2005 Dr. Alfredo Kohn Loncarica
2005-2009 Dr. Jorge R. A. Vanossi
2009-2013 Dr. Angel Alonso
2013-2017 Dr. Eduardo A. Castro
2017-2019 Dr. Angel Alonso

"FUNGAL HYPERSENSITIVITY IN NASAL PATHOLOGIES".

A.Alonso, A.B.Pomilio, S.R.Rodríguez, S.M.Battista, K.Mouchián, A.Vitale.

Div. Alergia e Inmunología. Laboratorio de Química y Bioquímica Estructural, CONICET, Depto de Bioquímica Clínica, Hosp. de Clínicas, 2da Cátedra de Microbiología, Facultad de Medicina, UBA.- Academia Nacional de Ciencias de Buenos Aires.-

Resúmen: se expone el papel que juegan varios hongos ambientales (Bipolaris, Curvularia y Alternaria) en la génesis de enfermedades nasosinusales, sus proteínas y hexosas, y la respuesta inmune desencadenada.
Palabras clave: sinusitis fúngica alérgica; Bipolaris, Curvularia, Alternaria; IgE e IgG; proteínas, hexosas; PRIST; RAST; vacunoterapia.

Summary: the role of several fungi is exposed; Bipolaris, Curvularia and Alternaria were studied; specific IgE and IgG were detected; PRIST and RAST techniques were performed; proteins and hexoses from the fungi were determined; immunotherapy was indicated as well as specific antifungal drugs.-
Key words: nasosinusal fungal pathology; outdoor allergens; antifungal IgE and IgG were detected; PRIST and RAST were done; immunotherapy and pharmacotheraphy.

Introduction.

Fungi are eukaryotic organisms that cause disease in healthy being preponderant their aggressiveness in immunocompromised patients. Fungal infection of the paranasal sinuses was described many years ago, although it remains a controversial pathology due to its pathogenesis, clinical picture and treatment.
In 1791, Plaignaud described a case of fungal maxillary sinusitis, and in 1893, Mackenzie, did the same by establishing the etiopathogenic discussion. His diagnosis progressed thanks to the advent of computed tomography and endoscopy.
In 1971, Mc Carthy and Pepys observed that 10% of patients with allergic bronchopulmonary aspergillosis (ABPA) had a nasal discharge similar to that produced by the bronchus. 40% of the 111 studied had radiology of maxillary sinusitis and developed Aspergillus fumigatus in nasal mucus cultures.
In 1976, Safirstein observed that nasal symptoms in ABPA occurred when receiving treatment with oral corticosteroids. That same year, Young referred to the case of a 15-year-old

swimmer with maxillo-ethmoidal sinusitis, nasal polyposis and proptosis of the left eye, and found that this was due to the extension of the fungal material from the sinus to the orbit.
In 1983, Katzentein noted the coexistence of asthma, nasal polyps, sinusitis and a secretion which he called "allergic mucin" in affected sinuses, which was rich in mucin filaments, eosinophils, neutrophils, Charcot-Leyden crystals, and fungal hyphae.
Since 1980, the cases described showed that the fungi of the Dematiaceae family more than Aspergillus were those related to fungal allergic sinusitis (SAF). [1-2-3-4-5-6-7].

Classification and clinical forms.

SAF is a form of sinusitis that both clinically and histopathologically resembles the ABPA and should be distinguished from chronic bacterial forms and other fungal sinusitis.
These are invasive and non-invasive and are subdivided into 4 distinct entities:
1): the acute fulminant; 2): the indolent chronicle; 3): the mycetoma, and 4): the SAF itself. [8-9-10-11-12].

1): the **acute fulminant** form is invasive, rapidly progressive and occurs in immunosuppressed by HIV and not by HIV. The fungi are mostly Mucorales (Rhizopus, Mucor and Absidia), but also by the species Aspergillus.
The fungus proliferates in the paranasal vessels with ischemic necrosis, mucosal and bone destruction, and hematogenous invasion of the orbit, brain and skin.
It occurs abruptly with fever, pain facial, decreased vision, headache, lethargy and coma.
Nasal signs include serosanguinolent mucus, granular with black necrotic plugs in the turbinates and the septum, with nasal or palatine perforation.
Neurological signs indicate poorly prognosis and can lead to death.
The diagnosis is confirmed by the cultivation of the fungus, the histopathology with fungal invasion, necrosis and neutrophilia.
It is treated with necrotic tissue resection, amphotericin B intravenous (0.8 - 1.5 mg / kg / day) and adequate management of the underlying disease.
2): the **indolent chronic** form presents tissue invasion in immunocompetent individuals, whether atopic or do not. It is slowly progressing as a chronic granulomatous infection that simulates a neoformation.
Histologically, there is evidence of bone necrosis with a LTCD4-Th1 / Th2 infiltrate, plasma cells, neutrophils, eosinophils and Langhans giant cells.
In crops, both Aspergillus and Dematiaceae species are found. It is treated with surgical debridement, tissue and bone removal plus amphotericin B (total dose: 2 g), or ketoconazole (3,3-6,6 mg / kg / day) or itraconazole (200-400 mg / day). It has a good prognosis. [13-14-15].
3): the **mycetoma** caused by Aspergillus fumigatus or aspergilloma or "fungus ball", is chronic and non-invasive. They suffer healthy non-atopic. With few symptoms it affects the maxillary antrum. Is a round mass with mycotic hyphae like a wet chalk. It is distinguished from allergic forms by the absence of eosinophils in the nasal mucus. It involves the excision of the fungal mass and the aeration of the breasts endoscopically. Cure in 100% of cases. [16-17-18-19].
4): **SAF:** they are usually adolescents or young adults with a long history of obstruction nasal, rhinohidrorrea and sneezes with poor response to drugs and attempts surgical procedures. Their average age is 27 years (8 ± 31), and they may also suffer postnasal drainage with polypoid formation that is exhibited by the nose. Rarely do they have visual disturbances, proptosis, cranial nerve palsy, epiphora, pain, edema and structural facial alterations (telecantus). Its clinic does not differ from that of perennial or persistent rhinitis.

Physicians at the Children's Hospital of Saint Louis (USA) in 1984 described the case of a girl 10 years old with a painful maxillary and nasal mass that grew and deformed the face nostril affected. It was thought a tumor pathology and after the debridement was made diagnosis of mycosis by the species Curvularia. SAF is frequently accompanied by asthma (33-50%) and although the association of SAF with ABPA is not a rule, 10% of the latter have Aspergillus in the nasal mucus. There is no association between SAF and hypersensitivity to AINEs. [20-21-22-23].

Laboratory findings.

They have focused on the parameters identified as abnormal in ABPA. These include: elevated eosinophil count, increased serum IgE, specific IgE antibodies, positive skin sensitivity for probably involved fungal antigens, and presence of IgG and specific serum precipitins. Elevated eosinophilia in more than 600 per mm3 occurs in 50% of patients. Unfortunately, there are no published studies yet linking eosinophil counts to disease development, but it is presumed to fluctuate with eosinophil activity, as in ABPA.

Patients have total serum IgE greater than 100 ng / ml and a subgroup of individuals have elevated levels (≥ 1000 ng / ml). There are positive skin tests and specific IgE antibodies against the culture material of the breasts. It is difficult to diagnose type I hypersensitivity in the form of prick-test or intradermorreaction, as well as RAST (radio-allergo-sorbent-test) to fungal antigens, due to the low viability and standardization of the extracts.

It is common for individuals to have positive skin tests with common aeroallergens of the habitat or anemophilous fungi and RAST equal to class 2 or higher. In some studies, an increase in specific IgG antibodies or the presence of serum precipitins against the fungal antigens involved has been reported. All this led to the development of appropriate witnesses to certify the presence of a specific IgE and / or IgG before and after specific vaccination with Bipolaris and Curvularia antigens isolated from patient samples and cultured by us in our labs, as well as the proinflammatory cytokine IL-2 and IL-4 dosages and receptor expression for the latter (IL-4R) before and after immunotherapy by assessing the biochemical changes induced by it.

Erythrocyte sedimentation is usually within normal ranges. If elevated, it is probably due to concomitant bacterial infection. [24-25-26-27-28]

In some studies, the patients were submitted to immunological evaluation including analysis of lymphocyte subpopulations and titration tests of cellular immunity. None presented evidence of immunodeficiency, diabetes or cystic fibrosis.

Mycology:

Culture and cytology of the mucus are essential for the diagnosis of certainty of the SAF. The fungi involved are from the family Dematiaceae (formerly Helmintosporium) which include Bipolaris sp., Drechslera sp., Alternaria sp., Curvularia sp., Exserohilum sp., Aspergillus sp., Rhizopus sp., Fusarium sp. and Chrysosporium sp.

They are dark pigment fungi typical of the soil, plants, tree trunks and water.

They were considered saprophytes and are identified with Gomori's silver-metamine staining being useful neither the May-Grünwald-Giemsa nor the hematoxiline-eosine.

Their slow cultivation makes it difficult to identify them because they can be considered as contamination.

One alternative is in situ hybridization (HIS) that by using known DNA fractions that are bind to a ribosomal RNA sequence of the fungus allows rapid identification.

If it is not possible to detect fungal elements, the diagnosis can not be confirmed.

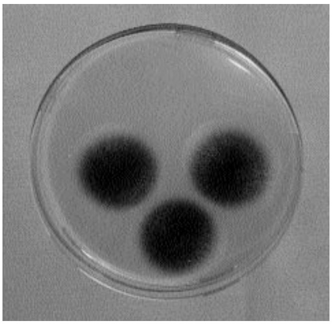

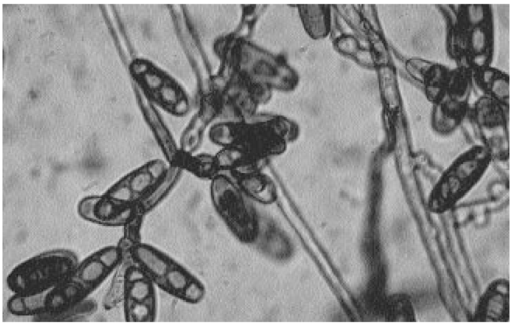

Figs. 1 and 2: Cultivation and microphotography of Bipolaris australiensis.

BIPOLARIS AUSTRALIENSIS and other pathological species.

Teleomorph: Cochliobolus sp.

The colonies of this one are of fast growth, diffuse, of gray color to blackish brown, Whose inverse image is flocosa of black color. Microscopic morphology shows the development of pigmented pale brown, pseudoseptant with conidia geniculate or in zig-zag of the thallus. Conidia are produced through pores in the wall of the conidiophore (Poroconidia) and are straight, spindle-shaped or ellipsoidal, rounded at both ends, smooth to finely rough and germinated only at the ends (bipolar).
The genus Bipolaris contains about 45 species that are subtropical and parasitic tropical plants, however, several species, in particular B. australiensis, B. hawaiiensis and B. spicifera are well documented as human pathogens.
Clinical manifestations include mycotic keratitis, subcutaneous Phaeohyphomycosis, sinusitis, peritonitis in patients on continuous ambulatory peritoneal dialysis (CAPD), infections and the widespread Feohifomycosis caused by Bipolaris sp.
reported in both normal and immunosuppressed patients.
Drechslera, Bipolaris, Curvularia and Exserohilum are closely related and the differentiation is based on a combination of characters including the conidia, the presence or absence of a protruding thread, the contour of the basal portion of the conidium and its thread, the point at which the tube originates in the germ of the basal cells and, in lower degree, sequence and location of the septa of the first 3 conidia. [29-30-31-32]

1. Colony appearance (on 30° C - Peptone glucose agar):
- Diameter: 80 mm in one week.
- Topography: smooth and extended.
- Texture: from cotton to felt.
- Color: gray-black. A white border is often displayed.
- Reverse: black.

2. Microscopic appearance at 30º C :
- Predominant characteristics: large conidia, oval, of brown color and thick wall, with multiple partitions. They occur in genicated conidiophores.
- Characteristics of conidia: large, from oval to elliptic, rounded at the ends, 14-40 x 6-11 μm

in diameter. 80-90% have 3 partitions, occasionally 4 or 5.

3. Differential diagnosis: with other species of Bipolaris, Exserohilum spp., Alternaria, Curvularia spp. of conidia, size and number of partitions. Exserohilum spp. Is distinguished by its outgoing and truncated thread. Helminthosporium spp. Is similar, but the conidiophores are not geniculate. Drechslera spp. Is also similar, but the conidiophors are not geniculate, it differs because it germinates at right angles to the axis of the spore. Curvularia conidia are curved.

4. Sexual status: Cochliobolus australiensis.

5. Clinical significance: It is a plant pathogen. Some cases of deep infection have been described in immunocompromised patients. Surgical removal of local lesions is important in all forms of pheochromocytoma. Corneal haemophomycosis: topical natamycin. Subcutaneous and sinus phaeohyphomycosis: itraconazole as a complement to surgery. Disseminated pituitary: voriconazole iv. or oral, itraconazole oral solution or amphotericin B-deoxycholate 1-1.5 mg / kg / day or equivalent doses of a lipid formulation. Alternatives: subcutaneous and sinus phaeohyphomycosis: amphotericin B-deoxycholate iv., or voriconazole.

Radiological findings:

If a patient presents a history and clinical suggestion of a chronic inflammatory sinus process with a simple pathological sinus plaque, the sectional image of the TAC may be a chance. Radiology minimizes diagnostic error as descriptive (localization).
The images in the SAF are non-specific: 1): multiple opacification of the paranasal sinuses to unilateral predominance; 2): thickening of the mucosa; 3): thinning of the breast wall and evidence of bone erosion. However, these changes are also observed in other infectious or tumor processes. In the tomography homogenous zones with different patterns can be observed: image of "starry ice" or serpiginous areas, of metallic density. Stamberger and colleagues describe 27 of 59 patients (46%) with metallic images compared to those of a foreign body, on the radiographs of patients diagnosed with SAF, attributed to the presence of phosphate and calcium sulfate in the center of the fungal mass. The presence of different degrees of bone erosion does not necessarily indicate tissue invasion. However, if the invasion is visible, as in intracerebral abscesses or optic nerve infiltration, they discard the diagnosis of SAF and are suggestive of acute sinusitis.
Nuclear magnetic resonance may be a complement to TAC in select cases that require additional information for an image. The radiologist can give a precise anatomical location, but the pathologist will have the last word.

Histopathology:

The mucoid impaction extracted from the paranasal sinuses was referred to initially as "allergic mucin". It is a thick material, with the consistency of the peanut butter and of yellow, brown or green color. Microscopically, accumulations of necrotic eosinophils and other picnotic cells are observed on a basophilic or eosinophilic amorphous background. Also appear Charcot-Leyden crystals that are hexagonal in the cross-sections or bipyramidal in the longitudinal. The direct visualization of the hyphae is quite rare; Are observed after staining or culture. There should be no evidence of tissue invasion in SAF.

In a study conducted in Phoenix, Arizona, by M.Shubert and D. Goetz with 67 patients suffering from allergic fungal sinusitis (the largest population described to date), in eight years of follow-up 4 key points were established to specify the histopathological diagnosis :

1). Allergic mucin, present at the macro and microscopic examination.

A- Macroscopy reveals black-brown to green material.

B- Mucin exudate stained with hematoxylin-eosine presents: a pale eosinophilic background, accumulations of picnotic eosinophils and Charcot Leyden crystals.

2). Both of them, too. The staining metamine positive plaque for fungal hyphae, but no hyphae are seen in the mucosa (with or without positive culture). Silver staining negative and positive culture for fungi.

3). A.- Hematoxylin-eosine staining of the sinus mucosa is characteristic for SAF and indistinguishable from the mucosal infiltrate in the asthmatic bronchus. Mucosa with eosinophil infiltrate, plasma cells and small lymphocytes (differential diagnosis with nonallergic eosinophilic rhinitis).

B. Absence of necrosis, granulomatous formation or giant cells.

C. Stromal edema.

D. Thickening of the basement membrane of the respiratory epithelium.

and partial scaling of respiratory epithelium.

E. Distension of mucous glands

4). Other fungal diseases are excluded.

Pathophysiology: The exact mechanism of SAF is under discussion. Histopathology similar to that of ABPA suggests that inhaled spores are trapped in the mucus where the fungus proliferates by releasing antigens and inducing an inflammatory Type I (IgE-dependent) or type III (Arthus-immune complexes).

With the authors we advocate type I since patients have positive skin tests for fungal antigens and aeroallergens with high total and specific serum IgE. Type III is debatable because the presence of specific IgG and precipitins is not correlated with an Arthus-type histopathology or general findings that justify it (vasculitis) and is the expression of the immune response to the mycotic antigen.

The inflammatory perpetuation by IgE plus cytokines (IL-1, TNF-α, IL-3, IL-4, IL-13) and locally released chemokines (RANTES) lead to nasal ABPA.

Since mycotic antigens may behave as superantigens, LTCD4-Th1 / Th2 in a HLA context can generate a chronification through the RcT-Vβ in addition to specific IgE with mastocytosis activation.

Diagnosis: based on the ABPA the authors propose these criteria:

1): presence of allergic mucin;

2): absence of bone or tissue invasion;

3): positive cultures for the fungus;

4): TAC characteristic of sinusitis;

5): immunocompetence;

6): nasal polyps;

7): atopy;

8): precipitins or specific IgG and

9): peripheral eosinophilia.

In our experience we suggest:
1): atopy;
2): TAC suggestive of SAF;
3): positive fungal culture;
4): allergic mucin and
5): nasal polyps.

These are the most frequent findings.

MATERIALS AND METHODS.

A): Antigens: extracts prepared by us using at the starting point of the culture of the Mycology Center of the School of Medicine that had been identified as Bipolaris australiensis, Curvularia and Alternaria alternata. The preparation methodology of the extract was the established by Frugoni and Hansen in their classic text. Their protein contents were determined by the Bradford technique giving a result of 13 mg / ml. An assessment of the presence of hexoses were positive and the antigens responsible for the immune response could be suspected as glycoproteins.

B): Patients: we studied 12 men derived from the Chair of Otolaryngology (Prof.Dra I.Kaimen-Maciel), aged between 18 and 29 years, with the diagnosis of SAF corroborated by the specialized studies and the mycological culture.
All of them were atopic, with a history of hereditary familiar and with a serum IgE total elevation of 230.50 ± 115.39 KU / L.

C): Skin tests: in all patients, intradermal reactions were performed on the face of the arm using disposable needles of 13 x 0.4 mm with 0.02 mL with the usual aero-allergens (mites, blattidae, cat and dog epithelia, pollens and anemophilic fungi), among which a marked difference (erythema-papule ≥ 20 mm) was found. The extracts of Bipolaris, Curvularia and Alternaria were injected with 8 mcg of pure protein each, sterilized by 0.22 μ Millipore filters. Controls were physiological solution pH 7.2 and sterile histamine phosphate diluted 1/1000. The reading was performed at 20 minutes measuring the generated erythema and papule. The response was coded as follows: 1 to 4 mm (+); 5 to 9 mm (++); from 10 to 14 mm (+++) and more than 15 mm (++++) from erythema-papule. The patients remained for 1 hour in observation to assess and control possible adverse systemic reactions in very sensitive subjects. The tests were performed by the morning and by the same person.

D): Radio and enzyme immunoassays: total serum IgE was determined by the ELISA following strictly the manufacturer's specifications (Phadebas, Uppsala, Sweden).
The results were expressed in KU / L.
In order to dose IgE and specific anti-Bipolaris, anti-Curvularia and anti-Alternaria- IgG, the RAST technique was developed following the steps established by Ceska. The results were expressed in Phadebas RAST Units (PRU / ml), originally in classes 0, 1, 2, 3, 4, 5 and 6, and actually, in their equivalents from 0 to 0.35; 0.35 to 0.70; 0.70 to 3.50; 3.50 to 17; 17 to 50; 50 to 100 and over 100 PRU / ml. IgG was expressed in International Units per milliliter (IU / mL).
Synthetically, the procedure was as follows: the fungi extracts constituted the solid phase covalently attached to the cellulose discs (SS547) with cyanogen bromide at pH 11 for 2

hours in an alkaline medium. The sites of the membranes that did not react were blocked for one hour by a 0.2 mol / L phosphate buffer, pH 7.5, bovine serum albumin to 5% and 2% Tween 20 in distilled water 1/5. They were then washed with 0.01% PBS-Tween and incubated overnight with a 1/8 dilution of patient sera. These reactants were washed with a buffer-blocker and the membranes incubated with 50,000 c.p.m. of anti-IgE (or anti-IgG) -I-125. (Pharmacia, Uppsala, Sweden) diluted in 1 mL of the buffer overnight, then washed and their radioactivity was measured in the gamma counter.
Controls of each experience with normal sera were always used. In order to ensure the specificity of the immune response, RAST-Inhibition according to the Gleich technique was applied. In addition to the absorptions of the antibodies with its specific antigen from dilution 10-6 to the concentrate were used. Other unrelated allergens, such as Lolium, Ambrosia, cat hair and pollens concentrates were used.
Serum dosages of IL-2 and IL-4 were performed with ELISA kits in sera stored at -20 ° C, whereas IL-4R levels were detected by RIA from an antiserum against the CD124 marked by us (kindly supported by Dr. Luis Mario Scavini) with I-125 following the method of Ceska. The sensitivities of the IL-2 equipment are of the order of 5 pg / mL, for the IL-4 of 1 pg or 10 mUI and for the IL-4R of 7 pg / mL. These devices detect between 0 and 4000 pg / mL of each cytokine and of the receptor (soluble or sIL-2, sIL-4 and sIL-4R forms). The purification of them has minimized the possibility of interference and false positives or negatives. (33-34-35-36-37)

RESULTS.

The 7 patients in the experimental group (vaccinated) discontinued all established medication At the time by the specialist (instillation of the sinuses with amphotericin-B or itraconazole). Nasal sprays with vasoconstrictors or corticosteroids were used if respiratory discomfort altered their quality of life. Anti-H1 antihistamines (e.g., loratadine,cetirizine) at the usual therapeutic doses for these cases of respiratory allergy were indicated.
They were induced an immunotherapeutic treatment with the extract of Bipolaris, Curvularia and Alternaria with a injection with progressive dilutions of the original extract with 13 mg / mL, starting from a dilution of 1 / 100,000 of that extract to the concentration of 1/10 in the third year. Every year venous blood sample to assess the presence of IgE and IgG isotypes as well as IL-2 and IL-4 cytokines and serum IL-4R.
The remaining 5 patients who refused immunotherapy received only symptomatic treatment with identical drugs, if the respiratory discomfort indicated it. Four of them relapsed their sinusopathy, and the otorhinolaryngologist had to institute local antifungal treatment.

However, they demonstrated their collaboration with the research project, by allowing annually the extraction of a blood sample to assess the presence of antibodies and specific anti-fungal IgG antibodies, and, of the cytokines or IL-4R for compare with samples drawn from patients in the experimental group.
The patients in the experimental group did not suffer recurrences of their pathology of origin asserted by the consultation with the Otorhinolaryngology Division over the 3 years of immunotherapeutic treatment.
Throughout the 3 years of specific immunotherapy with fungal extracts, serum IgE showed a decrease from 0.985 PRU / mL with an DE ± 0.455 PRU / mL to values of 0.29 PRU / mL with an DE ± 0.165 which means a $p \leq 0.02$ while the control group possessed from 1.02 PRU / mL with an DE ± 0.327 PRU / mL to 1.12 PRU / mL with an DE ± 0.318 PRU / mL with

a $p = 0.50$.
Both IgG-specific-anti-fungal and IL-2 cytokines, IL-4 and IL-4R, showed significant changes in patients vaccinated with a $p \leq 0.01$ to 0.001 while the unvaccinated group did not reveal changes of significance with a $p = 0.50$.
The test of precipitins (Ouchterlony) was negative not evidencing bands of precipitation, speculating that the IgG-anti-fungal detected does not belong to the precipitating antibodies, and, if presumably to the incomplete antibodies of Margni or to the IgG4, both with a possible protective role in the immunotherapy of the atopic as has been revealed in other human experimental models.
Immediate reading skin tests with fungal antigens performed at 3 years, revealed that in patients 1, 2 and 6 were negative while in the other 4 of the group vaccinated were still positive but weaker than the initial ones by measuring erythema and papulae. On the other hand, the patients in the unvaccinated group did not show any change in their local skin reactivity when tested with fungal antigens.
The cellular participation in the clinical improvement is assumed taking into account that, the immunotherapy activation of lymphocyte populations T and B, which, the LT-CD4-Th2 functionality is exacerbated with the production of their cytokines.
The decrease in the serum values of IL-2, IL-4 and IL-4R in this model is auspicious.
Another aspect that should be studied is the role of those metabolic products of the fungus (eg, proteases) that allow its colonization and perpetuation in the mucosa as was demonstrated in many research projects and some with other fungi such as Aspergillus fumigatus and Rhizopus nigricans. [35].

CONCLUSIONS AND DISCUSSION.

Conventional treatment of SAF is essentially medical.
If there is no tissue or bone invasion and patients do not require antifungal systemic drugs. Although in the ABPA oral antifungal drugs reduce symptoms, in the Dematiaceae conditions are poorly susceptible to itraconazole.
New therapies propose the use of topical or inhaled antifungal agents, as irrigation of the paranasal sinuses with amphotericin B or ketoconazole. The undisputed step and fundamental is the surgical debridement by endoscopy with removal of the fungal mass and sinus ventilation. The disadvantage is the high percentage of relapses after surgery.
Waxman divided the patients into 3 groups: a): immediate relapse in months; b): the late recurrence in years and c): prolonged remission. In the absence of an indicator that who will be well after the surgery are recommended the inhaled corticosteroids post-operative or orally at the rate of 0.5 mg / kg / day of prednisone for 2 weeks.
This is when it is decided to carry out specific immunotherapy with the mycotic antigen isolated from the patient and properly prepared and standardized for its correct vaccination.
The literature is contradictory since while Ferguson (1997) desensitized 4 patients they all got worse; Mabry (1998) vaccinated 9 patients and 6 of them improved markedly and did not suffer relapses.
Vaccinotherapy did not produce any adverse effects and allowed the discard of the medication as inhaled corticosteroids.
The prognosis of SAF is variable and the percentage of recurrences after surgery with and without steroids is high (32-100%). Endoscopic surgery of the breasts with aeration, removal of affected tissue, restoration of mucociliary clearance preserving normal anatomy provides immediate improvement of symptoms, but does not guarantee absence of relapses.

Therefore, it is considered that the incorporation of specific immunotherapy in all cases is justified to modify the inflammatory tissue and to avoid or reduce relapses.
SAF is essentially a new atopic allergic entity in which a family of fungi triggers and generates a chronic inflammation that responds to the biochemical patterns of atopics.
It has nothing to do with the other 3 forms of mycosis sinumaxillares described since they are developed in another context and are not producers of a LTCD4 / Th2 response but rather than granulomatous and LTCD4 / Th1.
Therefore, it is considered necessary to incorporate the extracts of Bipolaris, Drechslera, Curvularia and Alternaria to the battery of diagnostic skin tests and to study more deeply those patients that show remarkable skin reactivity to the extracts of the fungi routinely studied.
Our findings resurrect the classic academic controversies related to the role of fungi, bacteria and viruses in the genesis of allergic inflammation on a previous genetic predisposition.- [29].

BIBLIOGRAPHY.

1.- Albónico J.F., Tiraboschi I.N. : "La sinusitis fúngica alérgica". En Temas de Inmunoalergia, tomo 5, Edit. CTM, Buenos Aires, 2004, págs. 99-114.
2.- Campana N., Alonso A. : "La poliposis endonasal recidivante". En Temas de Inmunoalergia, tomo 5, Edit. CTM, Buenos Aires, 2004, págs. 57-97.
3.- Alonso A., Campana N.R., Albónico J.F., Mouchián K., Kaimen-Maciel I. : Aspectos inflamatorios de la poliposis endonasal recidivante (PENAR).
Prensa méd.argent., 2009 ; 96 (4) : 197-205.
4.- Allphin A.L. : Allergic fungal sinusitis : problems in diagnosis and treatment.
Laryngoscope, 1991; 101 : 815-820.
5.- Bent J.P. : Diagnosis of allergic fungal sinusitis.
Otolaryngol. Head Neck Surg., 1994 ; 111 : 580-588.
6.- Blitzer A. : Fungal infections of the nose and paranasal sinuses.
Otolaryngol. Clin. N. Am., 1993; 26 : 1007-1035.
7.- Brandwein M. : Histopathology of sinunasal fungal disease.
Otolaryngol. Clin. N. Am., 1993 ; 26 : 949-981.
8.- Carter K.D. : Ophtalmic manifestations of allergic fungal sinusitis.
Am.J.Ophtalmol,1999; 127: 2, 189-195.
9.- Clarke S.R. : Allergic fungal sinusitis.
J.La State Med.Soc., 1998; 150 : 6, 248-252.
10.- De Shazo R.D. : Diagnostic criteria for allergic fungal sinusitis.
J.Allergy Clin.Immunol., 1995; 96 : 24-35.
11.-Ence B.K. : Allergic fungal sinusitis. Am. J. Rhinol., 1990; 4 : 169-173.
12.- Folker R.J. : Treatment of allergic fungal sinusitis : a comparison trial of postoperative immunotherapy with specific fungal antigens. Laryngoscope, 1998; 108 : 1623-1626.
13.- Gourley D. : Allergic Bipolaris sinusitis. J.Allergy Clin.Immunol., 1990; 85 : 583-591.
14.- Katzenstein A.L. : Allergic Aspergillus sinusitis.
J. Allergy Clin. Immunol., 1983 ; 72 : 89-93.
15.- Mackenzie J.J. : Preliminary report on Aspergillus mycosis of the antrum maxillare.
J.Hopkins Hospital Bulletin, 1983 ; 4 : 9-10.
16.- Mabry R.L. : Immunotherapy for allergic fungal sinusitis : three years'experience.
Otolaryngol. Head Neck Surg., 1998; 119 : 6, 648-651.

17.- Millar J.W. : Allergic aspergillosis of the maxillary sinuses.
Thorax, 1981 ; 36 : 710-715.
18.- Mc Carthy D.S. : Allergic bronchopulmonary aspergillosis.
Clin . Allergy, 1971 ; 1 : 261-266.
19.- Morpeth J.F. : Allergic fungal sinusitis : an update.
Annals Allergy, Asthma & Immunol., 1996; 76 : 128-136.
20.- Mukherji S.F. : Allergic fungal sinusitis.
Radiology, 1998 ; 207, 2, : 217-222.
21.- Muntz H. : Allergic fungal sinusitis in children.
Otolaryngol. Clin. N.Am., 1996; 29 : 185-191.
22.- Nash D.R. : Allergic fungal sinusitis.
Immunol. Allergy Clin. N. Am., 1998 ; 18 : 695-710.
23.- Plaignaud M. : Observation sur un fungus du sinus maxillaire.
J. Chir (Paris), 1791 ; 1 : 111-116.
24.- Sánchez Sánchez B. : Allergic fungal sinusitis.
Rev. Alerg.Mex., 1999 ; 46 : 5, 145-150.
25.- Shubert M.S. : Evaluation and treatment of allergic fungal sinusitis.
J. Allergy Clin. Immunol., 1998 ; 102 : 387-394.
26.- Shubert M.S. : Evaluation and treatment of allergic fungal sinusitis.
Treatment and follow-up.
J. Allergy Clin. Immunol., 1998 ; 102 : 395-402.
27.- Waxman R. : Allergic aspergillus sinusitis : concepts in diagnosis and treatment.
Laryngoscope, 1987 ; 97 : 261-266.
28.- Shubert M.S. : Medical treatment of allergic fungal sinusitis.
Annals Allergy, Asthma & Immunol., 2000; 85 : 90-101.
29.- Ruiz Moreno G. : Lecciones de Alergia. Edit. López & Etchegoyen.
Buenos Aires. 1957.
30.- Alonso A., Albónico J.F., Tiraboschi N.I., Mouchián K., Pionetti C.H., Irañeta S.G., Kaimen-Maciel I. : Patogenia e inmunoterapia en la sinusitis fúngica alérgica (SAF).
Prensa méd argent., 2009 ; 96 (7) : 407-410.
31.- Bradford M.M. : A rapid and sensitive method for the quantization of microgram quantities of protein utilizing the principle of protein-dye binding. Anal.Biochem., 1976 ; 72: 248-260.
32.- Gleich G.J. : The radioallergosorbent test : its present place and future in the practice of allergy. Advances in Asthma and Allergy, 1975 ; 2 : 1-9.
33.- Berrens L. : Possible indirect binding of IgE in house-dust RAST. Ann.Allergy, 1979 ; 43 : (1) : 38-45.
34.- Gleich G.J. : Measurement of IgE in normal and allergic sera by radioimmunoassay.
Journal of Laboratory and Clinical Medicine, 1971 ; 77 : 690-699.
35. Irañeta S.G., Duschak V., Rodríguez S.M., Alonso A. : Serine proteinases with gelatinolytic activity in an Aspergillus fumigatus allergenic extract. J. Invest. Allergol. Clin. Immunol., 2002 ; 12 (4) : 257-262.
36.- Pomilio A.B., Battista S.M., Alonso A., Vitale A.A.: Valor de la micología como complemento de los análisis químicos, bioquímicos y palinológicos en las investigaciones forenses y paleoecológicas. Anales de la Sociedad Científica Argentina, 2018 (4): 33-60.
37.- Pomilio A.B., Battista S.M., Alonso A.: Micetismos. Parte 1. Sindromes con período de latencia tardía. Acta Bioquim. Clin. Latinoamer., 2018 (en prensa).

USING HIGH-RESOLUTION, TASKABLE REMOTE SENSING IMAGERY TO SUPPORT A SENSORWEB FOR THAILAND FLOOD MONITORING

Steve Chien,[*] David Mclaren[†], Joshua Doubleday[‡], Daniel Tran[§]
Jet Propulsion Laboratory, California Institute of Technology, Pasadena, CA, 91109-8099, USA

Veerachai Tanpipat[**], Royol Chitradon[††]
Hydro Agro Informatics Institute, Bangkok, Thailand

* Principal Investigator, Thailand Flood Sensorweb; also Senior Research Scientist, Artificial Intelligence Group, JPL/NASA, Pasadena; steve.a.chien@jpl.nasa.gov.
† Software Engineer, Artificial Intelligence Group, JPL/NASA, Pasadena.
‡ Senior Software Engineer, Artificial Intelligence Group, JPL/NASA, Pasadena; Joshua.doubleday@jpl.nasa.gov.
§ Senior Software Engineer, Artificial Intelligence Group, JPL/NASA, Pasadena; Daniel.q.tran@jpl.nasa.gov.
** Remote Sensing Specialist, Hydro and Agro Informatics Institute (HAII), Ministry of Science and Technology, Thailand.
†† Director of Hydro and Agro Informatics Institute (HAII), Ministry of Science and Technology, Thailand.

Space-based assets have been integrated into a sensorweb to monitor flooding in Thailand. In this approach, the Moderate Imaging Spectrometer (MODIS) data from Terra and Aqua is used to perform broad-scale monitoring for flood tracking at the regional level (250m / pixel) to generate flood detections/alerts. Based on these alerts The Earth Observing-1 Mission (EO-1) is autonomously tasked to acquire higher resolution (10m-30m/pixel) Advanced Land Imager (ALI) data and a number of other assets have imagery automatically requested, with yet further assets requested only in a semi-automated fashion. Based on these alerts, this data is then automatically processed to derive products such as surface water extent and volumetric water estimates in shapefile formats to enable interpretation in geographic information systems (GIS). These products are then automatically pushed to organizations in Thailand for use in damage estimation, relief efforts, and damage mitigation. To date Terra, Aqua, EO-1, Landsat, Ikonos, Worldview-1, Worldview-2, Geo-Eye-1, and Radarsat-2 have been utilized in some fashion in the sensorweb. We describe the overall autonomous detection, tasking, data acquisition, and processing sensorweb framework as well as ongoing work to extend to in-situ-sensor networks. We also document how the automatic triggering of targeted higher

resolution observations enables higher temporal and spatial resolution tracking of flooding events.

INTRODUCTION

Flooding has a tremendous impact on humanity and is worldwide in scale. Thailand (as well as greater southeast Asia) is particularly prone to flooding as observed during the 2010 and 2011 flooding seasons in Thailand. The Thailand flooding of October-November 2010 reported in MCOT (2010), Bangkok Post (2010), Wikipedia (2011) [1, 2, 3] was responsible for over 200 deaths, over $1.67 Billion USD damage, and affected over 7 million people [4]. The Thailand flooding in 2011-2012 was even more severe accounting for over 600 deaths and $45.7 Billion USD damage [5] as of February 2012 the full damage is likely to be considerably higher. Figure 1 shows band 7-2-1 MODIS imagery of Southeast Asia as provided by LANCE-MODIS that highlights the extreme extent of the flooding on a regional scale.
Understanding flooding, drought, hydrology, and the water cycle is a key scientific challenge. "The scientific challenge posed by the need to observe the global water cycle is to integrate in situ and space-borne observations to quantify the key water-cycle state variables and fluxes." [6].

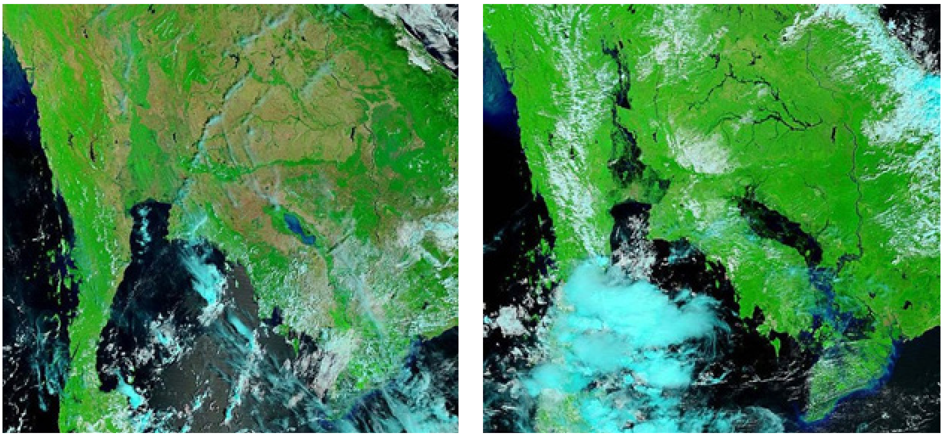

Fig. 1 Flooding in Southeast Asia, Fall 2011.
Left – Dry, March 6th, 2011. Right – Flooded, October 27th, 2011

Remote sensing can provide significant insight into flooding events such as the events in Thailand 2010 and 2011. Remote sensing data can be analyzed to provide flood alerts and flood products such as surface water extent maps and/or be combined with digital elevation maps to provide water depth information. These two in concert can provide valuable indicators for flood damage and water volume.

Sensorweb – The Concept

The sensorweb is a concept where a networked set of sensors is used to measure an environmental phenomenon. In the context of flooding, in our sensorweb concept (see Figure 2), the sensorweb constantly automatically assimilates available data from multiple sources to track flooding. This may be as easy as downloading the available data. Or it may mean active querying to determine if potentially contributing satellites are acquiring data and acquiring the data from relevant servers when available. Data acquisition may also involve downloading data from in-situ sensors via the internet. This data is used to constantly update our model of the flood state. All of these data can then be combined with hydrological models to perform *hindcasting* (estimation of flood parameters in the past to fill in missing times or areas), *nowcasting* (estimating the current flood state by using the model to fill in spatial gaps), and *forecasting* (using the model to predict which areas are at risk for future flooding).

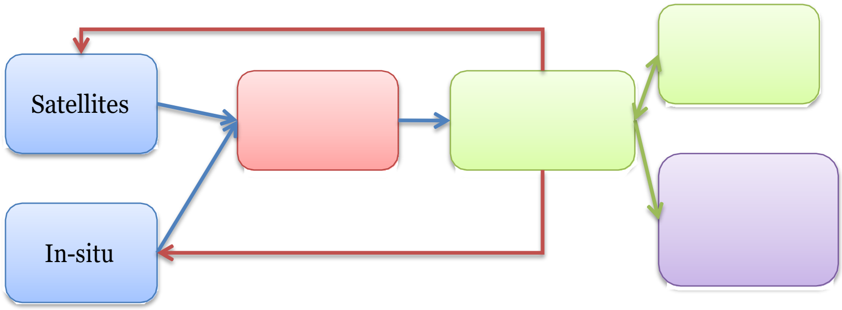

Fig. 2 Sensorweb Paradigm

When appropriate, the raw data and model are used to generate specific flood products for end users such as local, regional, and national authorities. These products may include surface water extent maps, water depth products, flood alerts for already inundated areas, and alerts for areas at future risk. When targetable satellite assets are potentially available, the sensorweb can automatically request data.

Key elements of the sensorweb concept are:

1. Automated detection of events or features of interest

2. Automated reconfiguration of the network (tasking) based on the automated detection (1.).

3. Automated Product generation and delivery

The key benefits of the sensorweb concept are:

1. Improved situational awareness of major events: by automating event detection, the sensorweb can enable 24/7 alert notification of major events of interest.

2. Improvement of the spatial and temporal resolution of data: The sensorweb triggers automatic acquisition of higher spatial resolution, swath-limited data in response to major events detected (e.g. 1. above). This higher resolution data can be used for a range of flood response purposes including damage estimation, mitigation, and allocation of response resources.

3. Better use of acquired data by assimilation and generation of information from data: the sensorweb automatically processes a wide range of data and provides it to the users in the format and with the analysis they need. Instead of getting a large number of uncorrelated raw imagery sources, the users have surface water extent, water depth, depth analysis geo-referenced data. Resultant shape filed can be ingested into their GIS systems where they can query the estimated water depth of any point. Providing the end user desired products increases the usability of the raw data.

Table 1: Space, Air, In-situ, Cyber Sensorweb Elements

	METHODS, ASSETS
DATA RETRIEVAL	Internet, various
DETECTION	In-situ sensors External reports Satellite monitoring, multispectral Satellite monitoring, radar Model predictions
TASKING	Space-based multispectral Space-based radar Model In-situ (stationary) In-situ (ground, mobile) Airborne
PRODUCT GENERATION	Hindcast, Nowcast, Forecast products, automatically computed by workflows.
PRODUCT DELIVERY	Internet, various

Table 1 above shows the actors and assets as envisioned in a notional sensorweb. While all of these assets may not yet be integrated, they all could provide improved capabilities to the end system.

II. Prior Work: Space-Based, In-situ, and Model-based Monitoring of Flooding

A number of satellites have been used to track flooding at a global or regional scale: most notably QuikSCAT (Quick Scatterometer), The Advanced Microwave Scanning Radiometer for Earth Observing System (AMSR-E), and Moderate Resolution Imaging Spectrometer (MODIS). QuikSCAT has been used by G. R. Brakenridge and his colleagues at the Dartmouth Flood Observatory [7] to track major flooding events. This method uses the change in backscatter to distinguish surface water from normal land areas. Averaging over longer time intervals (days) and comparisons against baseline data from prior years enables more accurate detections. While the use of scatterometer backscatter data enables detections even in the presence of clouds (a common difficulty as flooding, rain, and clouds all co-occur), this method relies on a running average technique thus reducing the timeliness of the detection (days).

The Tropical Rainfall Measurement Mission (TRMM) enables measurement of rainfall and therefore can be used as an indicator of flooding. AMSR-E and TRMM data have also been used to estimate stream-gauging values [8, 9] providing both a valuable indication of flooding and a key input to hydrological models. AMSR-E and TRMM are also not affected by cloud cover. Many projects have utilized MODIS to monitor flooding worldwide [9, 10, 11, 12, 13]. Again MODIS has moderate spatial resolution (250m+/pixel) so that its flood products are typically generated at a 250m per pixel resolution (although fractional pixel MODIS surface water extent has been demonstrated, e.g. [14]). One challenge in using optical sensors such as MODIS is occlusion from cloud cover that often occurs with flooding. These MODIS based flood-tracking methods utilize the MODIS multispectral capability. Flooded areas exhibit very low spectral response across a number of spectral wavelengths whereas clouds and land typically reflect more sunlight at certain wavelengths. Cloud shadows can often be hard to distinguish from surface water. MODIS based surface water detection methods often look at several overflights of data to address both cloud and cloud shadow difficulties.

However using this temporal technique causes a delay in detections. All of these global flood measurement techniques (e.g. AMSR-E, TRMM, MODIS) represent approaches to monitor flooding at a global scale.

Environmental Satellite (ENVISAT)/Advanced Synthetic Aperture Radar (ASAR) and Advanced Land Observation Satellite (ALOS) / Phased Array type L-band Synthetic Aperture Radar (PALSAR) have both been used to detect surface water extent from flooding. Synthetic aperture radar can distinguish between surface water and land areas due to the change in backscatter. Depending on the wavelength of the radar, surface roughness condition of the water (e.g. wind causing waves on the water surface) can cause difficulty in flood detection. The European Space Agency's Sentinel-1 is an example of a radar with strong applications to flood monitoring.

Landsat-7, (and more recently since the Thailand deployment, the Landsat 8-Operational Land Imager (OLI)) and Earth Observing One (EO-1)/Advanced Land Imager (ALI) can all be used to detect surface water using spectral methods. While these sensors provide higher resolution data (30m/pixel) their infrequent revisit rate and challenge with clouds limit their utility for global flood mapping.

Multi-sensor, multi-temporal methods for surface water extent mapping was the focus of an IEEE competition [15]. While utilizing all available data can certainly increase accuracy, often little data is available and designing a system to utilize multiple data sets can be challenging. In-situ sensors can also provide valuable information. In-situ sensors can provide point estimates of rainfall, water levels, and in some cases flow rates.

Hydrological modeling is an essential part of flood management. Hydrological models are typically grid-based water balance models that track incoming water from rainfall or from upslope, water lossage from evaporation or absorption, and outflow (downslope). Hydrological models are critical in that they enable tracking the movement of the water downstream and thus can provide warning as flood waters move from highlands to lower lying plains, a frequent occurrence in Thailand. All of the sources of data we have described in this section (e.g. satellite, in-situ) can be considered inputs to the hydrological models.

There have also been a number of applications of elements of the sensorweb paradigm to flood monitoring. The MSG geostationary satellite provides data every 15 minutes that can track surface water extent [16]. However this data is only 3km spatial resolution and more precise flood monitoring is desirable to enable finer measurement of water volumes and better estimates of damage.

Sensorwebs have also been applied to flood monitoring in Namibia [17]. This effort included flood mapping with EO-1 and Radarsat-1, use of Open Geospatial Consortium web service interfaces, use of the cloud to store and process data, and the use of mashup dashboards to overlay multiple data sources.

Experiment: A Sensorweb for Space-Based Monitoring of Flooding in Thailand

We have implemented and operated a space-based sensorweb to monitor flooding in Thailand. This sensorweb demonstrates key aspects of automation in data assimilation, event detection, triggering of further sensing, automatic derivation of analysis products, and automated delivery of such products.
We describe the several key steps of automation:

1. Automatic fetching and interpretation of data to enable rapid notification of events

2. Automatic request generation for tasking/data acquisition requests based on recognized events

3. Automatic and semi-automatic fetching, and automatic processing/interpretation of data to enable better (e.g higher spatial and temporal resolution), and automatic delivery of analysis products

Specifically we hypothesize:

1. that existing sensor systems can be leveraged in an automated for effective (sensitive enough to capture major flooding events), accurate (low false alarm rate) for regional flood monitoring

2. that tasking requests can be automatically generated off of 1. Above

3. that the data from 2. above can be (semi) automatically retrieved

4. that the data from 2. above can be automatically processed to derive end user products and delivered
That all of the above automation (1.-4. Above) results in significantly higher spatial and temporal resolution products of greater utility to the end user

A. The Thailand Flood Sensorweb – A Pilot Operational Sensorweb

We have operated a sensorweb to monitor flooding in Thailand for the 2010 and 2011 [18] flooding seasons (roughly beginning in May and ending as late as spring the following year). The core of this system uses the MODIS and EO-1/ALI sensors and leverages the unique automated tasking capability of EO-1. Other sensors including Worldview-1, Worldview-2, Geo-Eye-1, Ikonos, Landsat-7, and Radarsat-2 have been integrated in a less automated fashion (specifically manual tasking and data retrieval). These sensors and assets are combined with automated workflows to deliver satellite imagery, surface water extent products, and surface water volume products to relevant entities in Thailand. The success of this core system has built the foundation for ongoing work to add additional sensors and data products such as TRMM, river basin and sub-basin hydrological models, and data from in-situ sensor networks. Below we describe the core operational sensorweb and ongoing efforts to expand the sensorweb.

B. Automated Flood Detection Using MODIS

Our primary sensorweb flood alert mechanism is triggering via analysis of MODIS imagery. MODIS provides excellent temporal coverage (at least 2x per day daylight overflights). We

retrieve the subsetted United States Department of Agriculture - Foreign Agriculture Service (USDA-FAS) Indochina MODIS data in geotiff format from the MODIS rapid response site (originally rapidfire and now LANCE-MODIS). This imagery is then analyzed and surface water pixels compared to baseline dry season levels to detect flooding [18].
Specifically the workflow for the MODIS flood detection is as follows:

1. Twice per day, download the FAS Indochina subsetted MODIS data, at the time of operation this was from rapidfire.gsfc.nasa.gov, at the time of publication this system has been replaced by LANCE_MODIS. These are 250m MODIS band 7-2-1 geotiffs.

2. For a set of pre-specified target areas of interest, we process a 20km x 20km box.

3. For each target box, we first mask out permanent water bodies as determined by dry season data.

4. Next, to mitigate the occurrence of clouds, for each pixel location we trace backwards in the images until we find a cloud free pixel to score (allowing tracing back up to 8 images). This constructs a complete image.

5. Then for each pixel in the image not masked out as a permanent water body or for which there is no cloud free data, we compute the ratio of band 1 to band 2 (e.g. 620-670 nm / 841-876 nm) and apply an empirically derived threshold to separate the classes.

Figure 3 shows the band 7-2-1, surface water extent maps, and flooding scores (flooded and dry) for the Ayutthaya-Chao Phraya box north of Bangkok near the Chao Phraya River for 27 October 2011. At left is shown the band 7-2-1 image, and at right the surface water extent classification which blue indicating water, green indicating land, and white indicating permanent water mask.

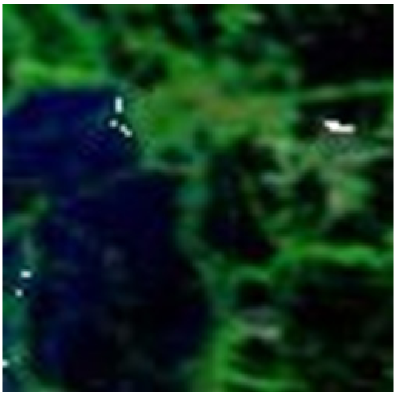

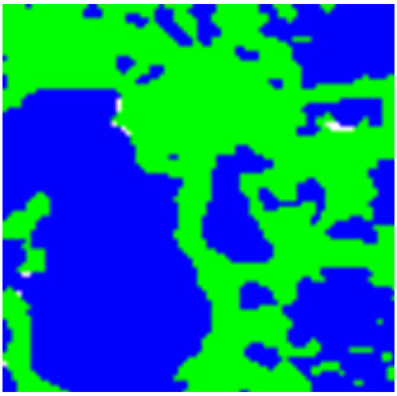

Fig. 3 MODIS Thresholding – Surface Water Extent
Ayutthaya-Chao Phraya TFS (October 27, 2011)
Pixel counts Cloud: 18 Water: 3662 Baseline: 25 Land: 3209

Figure 4 shows the band 7-2-1 RGB (at left) and surface water extent map (at right) derived from an entire FAS Indochina MODIS data showing the peak flooding 27th October 2011.

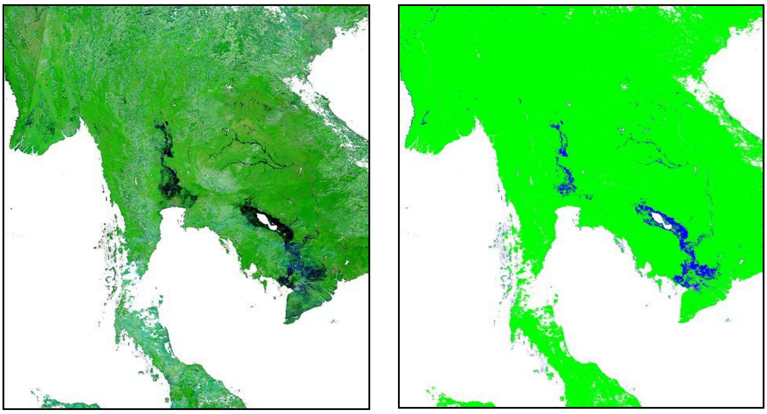

Fig. 4 MODIS Thresholding – Southeast Asia Region. Image credit: MODIS/LANCE-MODIS/GSFC/JPL Left – Composite of Indochina2 subset (October 27, 2011). Right – Surface Water Extent (Blue)

C. Automated Tasking of Response Satellite Imagery

The Earth Observing One spacecraft is the core of our sensorweb because of its automated tasking capability [19, 20]. EO-1 is automatically tasked from each MODIS flood detection/alert. The Thailand flood sensorweb MODIS alerts comprise a sensorweb campaign [19] within the EO-1 tasking system and therefore each alert can cause an observation request with an assigned mission priority. For each detection/alert EO-1 was tasked requesting Advanced Land Imager (ALI) Instrument imagery (30km wide swath, 30m spatial resolution multispectral, 9 bands 0.4-2.4 μ m spectral range).
Each tasking request for EO-1 is considered in the context of other competing tasking requests and spacecraft operations constraints [20] – including pointing, maneuver, data storage, thermal, and timing. The automated tasking system can accept requests 24/7 and continuously attempts to maximize acquisition of high priority images. Note that EO-1 also has an onboard flood detection system capability using the Hyperion sensor [21] that is not used for the flood sensorweb due to the limited Hyperion image swath width (7km vs. 30km).
Our flood detection and tracking system was also used semi-manually to request observations from other satellite assets by having flood detections/alerts generate emails to individuals with tasking authority for satellite assets. We also automatically search available imagery from both tasked and other satellite assets to find all available imagery of flooded targets including a wide range of assets: Landsat-7, Ikonos, Worldview-1, Worldview-2, Geo-Eye-1, and Radarsat-2.

D. Automated Estimation of Surface Water Extent in EO-1, Worldview-1, Worldview-2, Ikonos, Geo-Eye-1, and Landsat Imagery

We applied Support Vector Machine Learning (SVM) [22] techniques to learn classifiers to automatically detect flooded areas in EO-1, ALI, data [18] and Worldview-2 data [23]. Figure 5 shows surface water extent derived automatically using SVM classification methods from EO-1/ALI imagery. Figure 6 shows surface water extent from Worldview-2 multispectral data. Scenes of ALI and Worldview-2 data from regions of Thailand were collected and hand labeled for water (large lakes or catchments), developed areas, undeveloped ground, cloud, and finally cloud shadowed regions. In the interest of producing products that may be useful in flood mitigation, labels for ground and water were chosen aggressively through partially clouded observations. Labeling, training, validation (quantitative and qualitative) and kernel-parameter selection, was done through the Pixellearn tool [24].

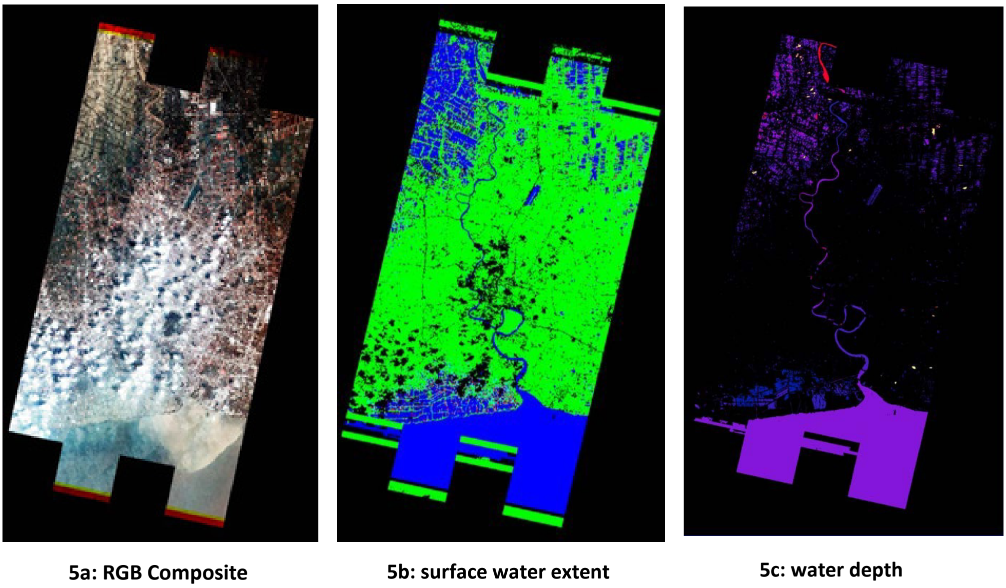

Fig. 5 Automated Interpretation of EO-1/ALI scene of Bangkok, Thailand, 31 October 2011.
5a (left): an RGB Composite
5b (center): surface water extent
5c (right): water depth

Several datasets (Worldview-2, Ikonos, Geo-Eye-1, Landsat-7 ETM) have been analyzed using band ratio surface water extent classification techniques. In this approach the ratio of the green to near infra-red spectral bands is thresholded to discriminate between land and water. Figure 6 (upper left, lower left, lower right) show automatically derived surface water extent maps from Worldview-2 imagery. Both the SVM and band ratio methods show good accuracy. Figure 7 (left, middle) show Geo-Eye-1 imagery and band ratio derived surface water extent product. Figure 8 (left, middle) shows Ikonos imagery and derived surface water extent product. Figure 9 shows the Landsat-7 surface water extent product.

6a: 6d:

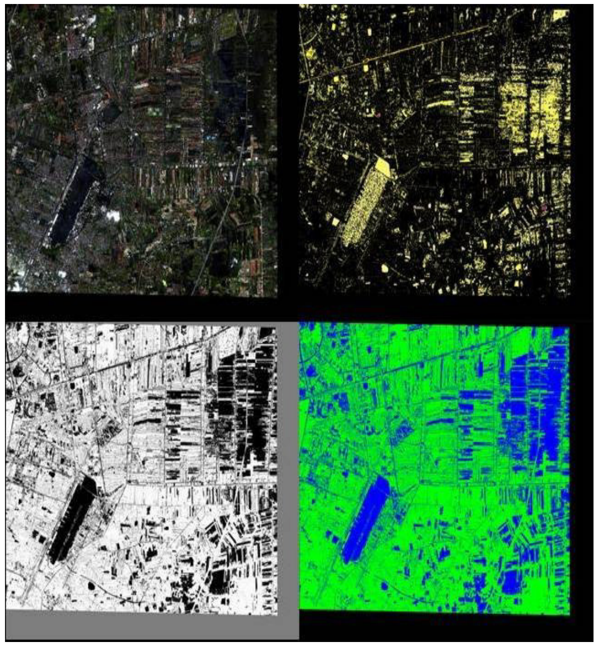

6b: 6c:

Fig. 6 WV-2 scene (Catalog ID: 2020010090403A00) taken November 3, 2011, North of Bangkok, Thailand.
Don Muang Airport is visible at left (west).
6a (upper left): RGB composite
6b (lower left): band ratio water extent map: black=water,
6c (lower right): SVM surface water extent map: green=land, blue=water,
6d (upper right): water depth map: pale yellow = 0 meters, blue = 9m

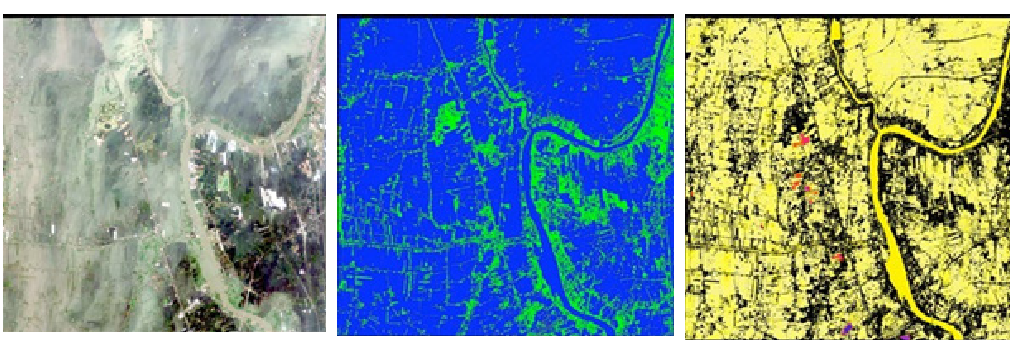

Fig. 7 GeoEye-1 scene of region north of Bangkok (image identifier: 20111111035723016030316093062- 011111103572301603031609306_001) acquired November 11, 2011.
7a (left): RGB
7b (middle): surface water extent map calculated by thresholding G and NIR bands: blue = water, green = land (middle);
7c (right): water depth map: pale yellow = 0 meters, blue = 13.7 meters (right).
The water volume in the image is calculated as 465,000,000 m3 at an average depth of 1.43 meters; however, this includes part of the Chao-Praya river.

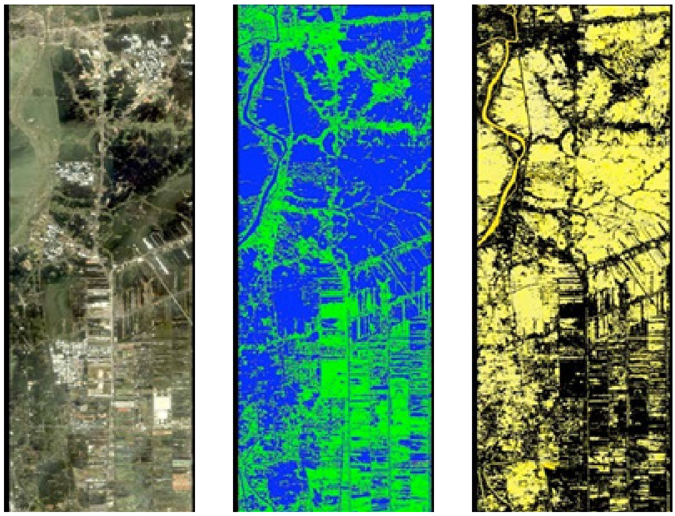

Fig. 8 IKONOS scene (image identifier: 20111104035450300000116241782000082842201THC) acquired over region north of Bangkok on November 4, 2011.
8a (left): RGB
8b (center): surface water extent map calculated by thresholding Green and NIR bands: blue = water, green = land (center);
8c (right): calculated water depth map: pale yellow = 0 meters, blue = 12.5 meters.
The water volume in the image is estimated as 321,400,000 m3 at an average depth of 1.30 meters.

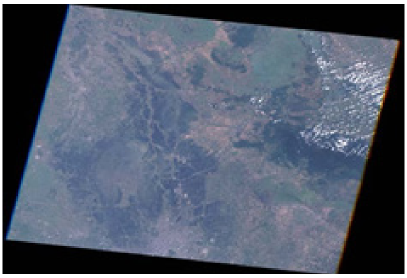

9a: True color RGB Landsat-7 ETM scene with gap filling from 17 Nov 2011. Bangkok (and flooded Don Muang airport) are visible on south side.

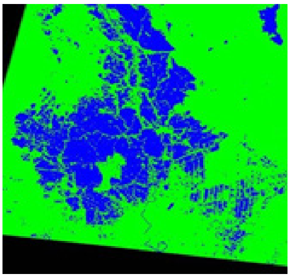

9b: Surface water extent map 17 Nov 2011 classified using green / near infra-red ratio: blue = water, green = land, black = no data; only includes area within bounds of DEM.

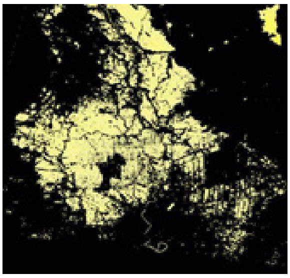

9c: Water depth map derived from gap-filled imagery from 17 Nov 2011. Maximum water depth = 77.3 meters (tiny spot), average flooded pixel depth = 1.79m, total volume = 9,842,000,000 m . # of distinct water bodies: 1,761.

Fig. 9 Landsat-7 ETM Interpretation

For the Thailand flood monitoring project all of the satellite imagery was used to directly extract surface water extent maps. This is only a moderately challenging task from good multispectral data. From our assessment, all of the remote sensing products (e.g., ALI, WV-2, Ikonos, Geo-Eye, and Landstat-7) were more than adequate for this task. Therefore the

only discriminating factors were: geographic availability, temporal availability, and spatial resolution.
The data access and surface water extent product workflow is shown below.

1. retrieve data automatically (EO-1/ALI, Landsat-7) or semi-automatically (WV-2, Ikonos, Geo-Eye 1)

2. apply SVM and/or band ratio to generate surface water extent (SWE) products

3. stage SWE products to archive (for delivery with surface water depth products).

Table 2: Satellites used and their capabilities

Satellite/Sensor	Green Band (nm)	Near IR Band	Temporal Frequency	Spatial Resolution
EO-1/Hyperion	550	860	Tasked	30m
EO-1/ALI	525 – 605	845 – 890	Tasked	30m
Worldview-2	510 -580	770-895	Tasked	2m
Ikonos	506 - 595	757 – 853	Tasked	4m
Geo-Eye-1	510 - 580	780 - 920	Tasked	2m
Landsat-7 ETM+	525 - 605	750 - 900	Every 16 days	30m

E. Automated Derivation of Water Volume from Surface Water Extent and Digital Elevation Information

We have created a workflow that uses surface water extent classification results from a sensor (including MODIS, ALI, WV2, Landsat, or Radarsat2 raster GeoTIFFs), calculates pixel heights using a digital elevation model (DEM), and estimates the depth of flood-water pixels by estimating their elevation from their boundary. Because the program reads classified images as input, it generalizes well to a large suite of instruments: any classification data that can be saved in a GeoTIFF can be used in this approach. We tested this system using scenes of flooding in Bangkok during October-November 2011. We obtained a DEM of the Bangkok & Ayutthaya region of Thailand, with 5m horizontal and 1m vertical resolution, from Thailand's Hydro and Agro Informatics Institute (HAII).
For the Thailand sensorweb, we automatically receive ALI data acquired by the EO-1 satellite along with the SVM derived surface water extent (as described above). Unfortunately, the ALI images are poorly registered, often requiring manual registration of the images by fixing them against shapefiles of road and permanent water body data using ArcGIS.
We automatically acquire and process data from a range of other sources including Radarsat-2, Worldview-2, Ikonos, and Geo-Eye-1 (sole manual steps are retrieval for some products requires manual login and registration of ALI used to require manual step – however this has since ben automated) . For these datasets

The procedure used to estimate water depths of flooded pixels is roughly as follows (see [25] for further details):

0. Retrieve surface water extent maps (see above)

1. Identify all land, water, and no-data pixels from classification results.

2. Identify all (land or water) pixels at a land-water boundary.

3. Identify all connected bodies of water within the image.

4. For all water and boundary pixels (i,j), estimate the height of the pixel h[i,j], using the following procedure. Given a geolocated DEM and the input classification image's horizontal resolution R (in meters), we estimate height by finding the nearest pixel in the DEM corresponding to the lat-lon location of (i,j) in the classification map, constructing a box around this pixel with side length R, and setting h[i,j] to the average of all the DEM pixel values found inside this region.

5. For each water body f, estimate water elevation:

6. Store a list of elevations of boundary pixels for the feature, boundary[f]

7. Initialize feature elevation E[f] = 0

8. if (length(boundary[f]) > 0) then E[f] = mean(boundary[f])

9. For all water pixels (i,j), calculate depth:

10. if(f[i,j] > 0) then d[i,j] = max(0, E[f[i,j]] – h[i,j])

11. Deliver both surface water extent and water depth products to registered users.

In our case this included HAII and thaiflood.com

The workflow outputs a GeoTIFF giving per-pixel water depth, with the same resolution and geolocation as the input classification map. As an example, for Worldview-2, for the scene shown in Figure 6a the surface water extent is shown in Figures 6b and 6c and the water depth in Figure 6d.
Several factors can impact the accuracy of this method. The classification of images itself is not perfect - not all land and water pixels can be reliably identified. Additionally, accurate geolocation in the classified output is essential to acquire elevation information from the DEM and derive accurate water depths. In the DEM itself, 1m jump in elevation represents a very large change compared to the roughly 2m average elevation for the city of Bangkok. The DEM data is also noisy; regions that would be expected to be flat in practice can be a mixture of pixels that differ by 1m in elevation. An elevation model with higher resolution would reduce noise and error in the water depth results.
It is also difficult to decide what to do with cloud or cloud shadow pixels, since it is unknown if these are flooded or not. It would be desirable to determine the status of these pixels based

on the status of their neighbors. Currently, cloud pixels are treated as if they contain no data.

Finally, this method assumes that water level can be inferred by equating it with the elevation of surroundings, but this may not necessarily be true in urban environments.
The volumetric water estimation techniques have been applied to EO-1/ALI (Figure 5), Worldview-2 (Figure 6), Geo-Eye-1 (Figure 7), Ikonos (Figure 8), Landsat,-7 (Figure 9) and Radarsat-2 (Figure 10) (which has a shapefile product). Worldview-2, Ikonos, and Geo-Eye data enabled most precise volume estimation from its high spatial resolution (2m/pixel). Radarsat-2 highlights the all-weather strengths of radar. Figure 9 shows the original Radarsat- 2 Shapefile product. In order to reuse our general workflow we rasterize this then use our general workflow to estimate water volume. Landsat highlights the multi sensor broad swath applicability of the techniques. Figures 8 shows Landsat-7 ETM-based tracking of flooding. We show gap-filled RGB, surface water extent, and water depth derived information, all derived from a Chao Phraya scene from 17 Nov 2011.

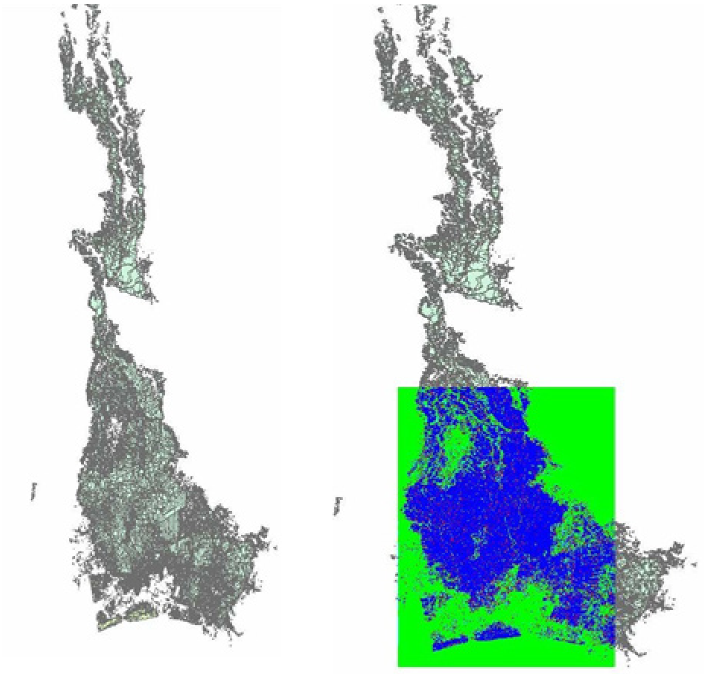

Fig. 10a (Left): Radarsat 2 polygonal surface water extent map. The shapefile extends all the way from Bangkok to northern Thailand. The image was taken November 11, 2011.
Fig. 10b (Right): Rasterized water extent map: blue = flood water, green = land or permanent water.
Generated within boundaries of Bangkok DEM, 25 meter resolution.

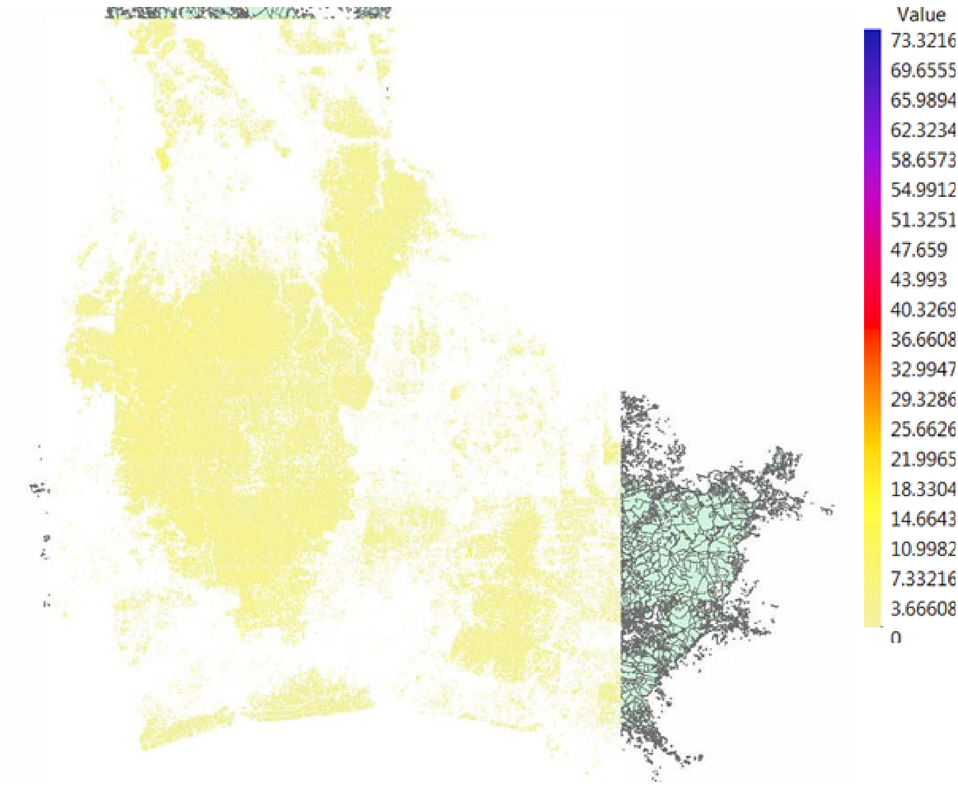

Fig. 10c: Radarsat-2 derived water volume. Zoomed in on water depth map, with scale at right. Maximum depth is given as 73 meters, but depths this extreme occur only in very small areas. Average depth of these pixels is 1.47 meters. The pale yellow pixels vary in depth up to about 3.5 meters. Total volume within this region estimated as 10,801,000,000 m^3.

F. Implementation

All of the sensorweb software runs at servers located at the Jet Propulsion Laboratory, California Institute of Technology (JPL). As indicated in the preceding sections, MODIS data is downloaded from the LANCE-MODIS site to JPL where it is processed for flood detection. Relevant imaging requests are generated and transmitted electronically to the EO-1 tasking system resident at JPL [20]. Response data is pulled automatically and semi- automatically from specific server sites to JPL and is then automatically processed into surface water extent and water depth products on JPL servers. These products are automatically electronically delivered from JPL to the Hydro Agro Informatics Institute (HAII) for access by and delivery to end users.

III. Experience using the Sensorweb in 2011-2012

We first deployed pieces of the sensorweb in the 2010 flooding season and added further capabilities in the 2011 flooding season. Working with authorities such as HAII, we identified 52 key monitoring sites in the Thailand region. From October 2011 through December 2012 we operated the Thailand flood sensorweb.
During this period, we have directly tasked over 50 ALI scenes during the extended flooding.

For some of these acquisitions manual direction via user defined site priority influenced the tasking (via coordination with Thai authorities). During this time Worldview-2, Geo-Eye-1, Ikonos, Landsat-7, and Radarsat-2 acquired over 100 additional scenes that were used with the sensorweb to produce surface water extent and water volume products.

Using mostly automated workflows, the sensorweb enabled rapid targeting, processing, product generation, and electronic delivery of products to relevant organizations in Thailand via HAII and Thailflood.com. The only manual effort involved specific ALI image to digital elevation map registration and some tasking and data delivery for commercial sources. The end products were used for a range of purposes in flood response, tracking, and damage estimation.

As of March 2017 the Earth Observing One mission was decommissioned – the sensorweb described continued operations until this time but commercial remote sensing assets were not triggered post 2013.

Table 3: Implemented Sensorweb Automation Elements In Thailand Flood Sensorweb Pilot

Sensorweb Element	Methods, Assets	Implemented in Thailand Flood Sensorweb
Data retrieval	Internet	MODIS[f] EO-1/ALI[f] Landsat[f] Worldview-2[p] Geo-Eye-1 [p] Ikonos [p] Radarsat-2[m]
Detection	In-situ sensors	-
	External reports	Web-based input
	Satellite monitoring, multispectral	MODIS[f]
	Satellite monitoring, radar	-
	Model predictions	-
Tasking requests	Space-based multispectral	EO-1/ALI[f] Worldview-2[p]
	Space-based radar	-
	Model	-
	In-situ	-
	Airborne	-
Product Generation	Hindcast, Nowcast, Forecast products	Nowcast – surface water extent[f], Nowcast - water depth map[f]
Product Delivery	Internet, various	Electronic delivery of SWE and depth to HAII[f] and thaiflood.net[f]

f – Fully Automated. p – Partially Automated m – Manual - - Not Implemented

A. Evaluation of the Experiment Criteria

Specifically we evaluate several hypotheses.

Hypothesis 1: that existing sensor systems can be leveraged in an automated for effective (sensitive enough to capture major flooding events), accurate (low false alarm rate) for regional flood monitoring.
Evaluation of Hypothesis 1: This hypothesis has been demonstrated. In the deployed Thailand flood sensorweb we have successfully automated data access via automated fetch from LANCE-MODIS, and automated major flooding event notification via automatic interpretation of this MODIS data and alert notification via the internet. Our flood detection algorithms were first validated on historical data, with parallel validation of the algorithms by both HAII hydrology and JPL automation teams. Additionally, early execution of the system was closely checked, with alerts validated by external sources (e.g. news reports, in-country personnel) and the system was deemed highly reliable.

Hypothesis 2: Pointable satellite assets could be automatically, effectively tasked from above generated alerts.
Evaluation of Hypothesis 2: This hypothesis has been partially validated. Significant numbers of EO-1/ALI images were automatically tasked. Additionally, via collaboration with DigitalGlobe we executed an email imaging request notification interface to WV-2, however this did not constitute a fully automated, electronic path. Several other satellite tasking pathways were investigated but never were implemented.

Hypothesis 3: that followup imagery (and alternate nadir pointing imagery) can be automatically retrieved for analysis.
Evaluation of Hypothesis 3: This hypothesis has been partially validated. For EO-1/ALI and Landsat data retrieval was fully automated. For several other sources (WV-2, GeoEye, Ikonos) we only received credentialed login access which could not be automated due to security restrictions. Therefore periodic, manual login was required to retrieve data.

Hypothesis 4: High resolution data can be automatically processed to derive end user products and automatically delivered to end users.
Evaluation of Hypothesis 4: This hypothesis was mostly validated. For all of the retrieved data products we were able to implement automated workflows to derive surface water extent and water depth products. The sole manual step was geo-location of ALI data which has since been corrected with the rollout of a USGS/GSFC EO-1/ALI improved geo-located product using the Landsat base map.

Hypothesis 5: The above sensorweb can provide improved spatial and temporal resolution tracking through the above automation.
Evaluation of Hypothesis 5: This is the most important hypothesis and it has been validated. The sensorweb products seamlessly combine multiple satellite measurements to provide higher spatial resolution and temporal resolution coverage of flooding events.

Figure 11 below shows the spatial and temporal resolution of delivered sensorweb products during the major flooding event on the Chao Phraya River near Bangkok 27 May 2011 to 17 July 2011. Landsat has data availability on a 16 day cycle with 3 images. EO-1 ALI was tasked to acquire 7 images. Therefore due to the sensorweb there were 10 products of 30m resolution available rather than 3 without the sensorweb.

Figure 12 below shows the spatial and temporal resolution of delivered sensorweb products during the major flooding event on the Chao Phraya River near Bangkok Thailand October – December 2011. Again Landsat is generally available at 16 day repeat but two images were not available for this time period. Also, three Worldview- 02, one Ikonos, One Geo-Eye and one Radarsat images were acquired and retrieved. However, the vast majority of the data coverage is from the automatically tasked EO-1/ALI that acquired 17 images during this flooding event. As the graphs show, without the tasked imagery a much lower spatial (MODIS 250m imagery twice daily), or at 30m lower temporal resolution (Landsat every 16 days) would only have been available. Nominally this would have been 5 Landsat images, but in actuality only 3 were available. So for this specific flooding episode without the sensorweb there would have been easy access to Landsat only (3 images) but instead there was access to 3 Landsat + 3 Worldview-2 + 17 EO-1 ALI + 1 Ikonos + 1 Geo-Eye + 1 Radarsat = 26 images.

Figure 13 below shows the available 30m or better spatial resolution imagery for continued flooding from January 2012 through March 2012 for continued flooding on the Chao Praya River near Bangkok Thailand. For this time period there are 5 Landsat-7 images, 10 EO-1/Ali images, two Worldview-2 images and one Geo-Eye image. Therefore for this specific flooding episode without the sensorweb there would have been 5 images, but with the sensorweb there were 5+10+2+1=18 images.

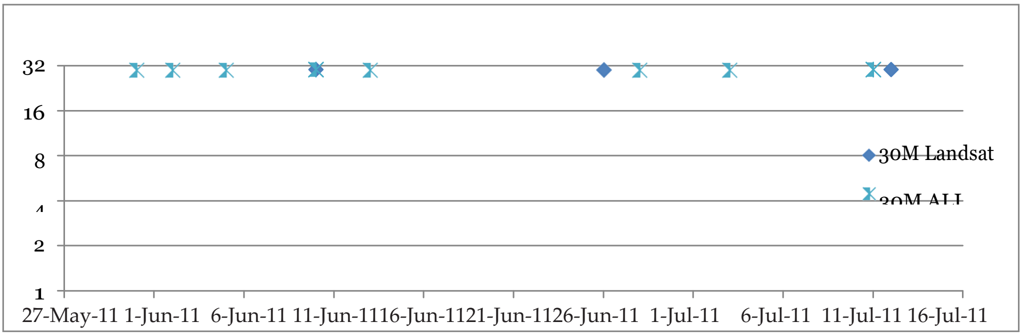

Fig. 11: Available 30m or higher spatial resolution data for Thailand Flooding 27 May 2011 through 16 July 2011.

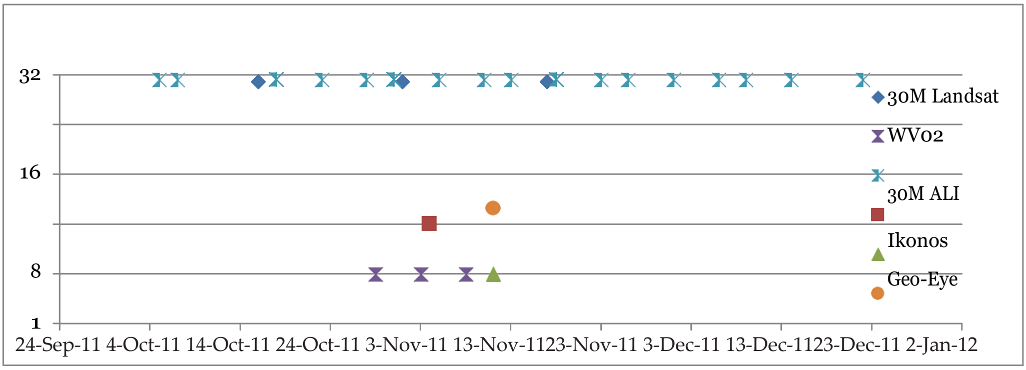

Fig. 12: Available 30m or higher spatial resolution data for Thailand flooding October through December 2011.

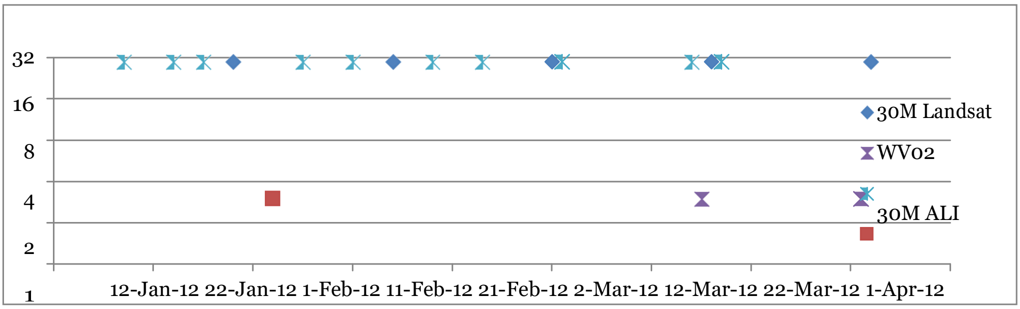

Fig. 13: Available 30m or higher spatial resolution data for Thailand Flooding January through March 2012.

Table 3 below highlights the increased number of images available as well as the increase in temporal resolution for the flooding events described.

Table 4: Summary of Gains from Sensorweb Coverage of Three major flooding events

Flooding event	Number of images without sensorweb	Number of images with sensorweb	Largest gap (in days) without sensorweb	Largest gap (in days) with sensorweb
Chao Phraya May – June 2011	3	10	16	15
Chao Phraya Oct – Dec 2011	3	26	43	9
Chao Phraya Jan – March 2012	5	18	16	12

B. Evaluation of the Experiment Criteria

HAII has developed and calibrated hydrological models for Thailand based on Soil and Water Assessment Tool (SWAT). This effort has used hydrological data from 2001-2009, 2009 land cover maps and 30x30m Digital Elevation Map. As of early 2012, HAII has completed hydrological models of all 25 major river basins in Thailand. Currently 10 river basins (mostly in the North and Northeast of Thailand) are operationally calculating monthly and weekly runoff utilizing script-based workflows to update input data from HAII's database, calculate runoff, and generate hydrologic maps automatically. The results are shown in the temporary website [26]. Additionally, an operational flood forecasting model for the Chao Phraya River basin is using another hydrological model, the North American Mesoscale (NAM) model - a lumped, conceptual rainfall-runoff model from the Danish Hydrologic Institute (DHI) to compute the daily runoff. For incorporation of weather data into these models, the HAII uses the Weather Research and Forecasting (WRF), Regional Atmospheric Modeling System (RAMS), Regional Ocean Modeling System (ROMS), and Coupled WRF-ROMS (3x3 km).

All of the hydrological models are used to manage the water resources in the 25 river basins

in Thailand. For this purpose they are integrated with the ARC/GIS V. 10.0 software under GIRD modules.
These hydrological models are used for several applications:

0. Water Resources Model (Mike Basin) for Dams and reservoirs management

1. River Model (Mike 11) for water flow management.

2. Flood Model (Mike Flood) for flood management.

Current efforts focus on integrating the hydrological model data into the sensorweb providing critical hindcasting (damage assessment), nowcasting, and forecasting to enhance flood monitoring, mitigation, and response.

HAII has developed an in-situ sensor network to monitor of hourly rainfall, weather parameters and water levels in main rivers. Throughout the country HAII is currently operating 774 automatic weather stations monitoring hourly rainfall, temperature, relative humidity, solar radiation, ground wind speed and air pressure and another 224 water level stations monitoring water level in main rivers every 10 minutes. The data are streamed to HAII via GPRS (General Packet Radio Service) under RS232 standard connection and publicly available at www.thaiwater.net. Those telemeters are being maintained by HAII and local contractors.

These in-situ data can directly inform the flood sensorweb for tracking flooding with timely information to feed both hydrological models and to be fused with more broad scale remote sensing data as could be seen in HAII's flood sensorweb flowchart below. Current efforts are directed at integrating this high temporal resolution, all weather in- situ data stream with the broad spatial coverage, sparse temporal resolution remote sensed (satellite) data.

Additional efforts are ongoing to integrate additional satellite data into the sensorweb. Fore example, weather satellites can provide valuable inputs into forecast models and flood tracking. AMSR-E, TRMM and GSMaP can also provide all weather river runoff and rainfall data. Efforts to integrate such sources are underway.

IV. Conclusions

We have described the deployment of a primarily space-based sensorweb to monitor and track flooding in Thailand. First, the Thailand Flood Sensorweb has demonstrated significant automation in: detection of events, automatic retrieval of data, automatic interpretation of data and generation of end user products, and in satellite retasking. This automation has been demonstrated to significantly enhance spatial and temporal resolution of flood monitoring. Future proposed work to integrate in-situ sensors and hydrological models offers additional benefits.

Funding Sources

The Jet Propulsion Laboratory Sensorweb work described was funded under the NASA Advanced Information Systems Technology Program, Earth Sciences Technology Office (ESTO) and by the Earth Observing One Mission.

Acknowledgments

Portions of this work were performed by the Jet Propulsion Laboratory, California Institute of Technology under contract with the National Aeronautics and Space Administration.

References

[1] MCOT – Ministry of Communication of Thailand, 19 November 2010, Available online: http://www.mcot.net/cfcustom/cache_page/131902.html (accessed on April 2012).
[2] Bangkok Post. FTI: Damage tally B50bn. Available online: http://www.bangkokpost.com/business/economics/204512/fti-damage-tally-b50bn (accessed on Nov 2010).
[3] Wikipedia. 2010 floods in Thailand and north Malaysia. Available online: http://en.wikipedia.org/wiki/2010_Thai_floods (accessed on March 2011).
[4] CNN. Death toll in Thailand flooding rises to 206. Available online: http://edition.cnn.com/2010/WORLD/asiapcf/11/13/thailand.flooding.toll/ (accessed on Nov 2010).
[5] World Bank. Thailand, Country at a Glance. Available online: http://www.worldbank.or.th/WBSITE/EXTERNAL/COUNTRIES/EASTASIAPACIFICEXT/THAILANDEXTN/0,content MDK:23067443~pagePK:141137~piPK:141127~theSitePK:333296,00.html (accessed on February 2012).
[6] National Research Council (NRC). Earth Science and Applications from Space: National Imperatives for the Next Decade and Beyond. National Academy of Science Press, 2007.
[7] DFO – Dartmouth Flood Observatory, Available online: floodobservatory.colorado.edu (accessed on February 2012).
[8] Brakenridge, G.R.; Nghiem, S.V.; Anderson, E.; Mic, R. Orbital Microwave Measurement of River Discharge and Ice Status. Water Resources Research, Volume 43, 2007, W0405.
[9] Brakenridge, G.R.; Anderson, E. MODIS-Based Flood Detection, Mapping, and Measurement: The Potential for Operational Hydrological Applications. Transboundary Floods, Proceedings. Of NATO Advanced Research Workshop, Springer, 2005, pp. 1–12.
[10] Brakenridge, G.R.; Nghiem, S.V.; Anderson, E., Chien, S. Space-based Measurement of River Runoff. EOS, Transactions AGU, May 2005, Volume. 86, Number 19, pp. 185-192.
[11] Carroll, M.; Townshend, J. R. G.; Dimiceli, C.; Noojipady, P. A New Global Raster Water Mask at 250 Meter Resolution.
International Journal Digital Earth 2009, Volume 2, Number 4.
[12] Carroll, M. L.; DiMiceli, C. M.; Townshend, J. R. G.; Sohlberg, R. A.: Noojipady, P. (ongoing), MODIS Flood Maps, University of Maryland, College Park, Maryland.
[13] GDACS. Global Flood Detection System, Version 2. Available online: http://old.gdacs.org/flooddetection/ (accessed on June 2012).
[14] OAS, NRT Global Flood Mapping. Available online: http://oas.gsfc.nasa.gov/floodmap/ (accessed June 2012).
[15] Li, S.; Sun, D.; Goldberg, M.; & Stefanidis, A. (2013). Derivation of 30-m-resolution water maps from TERRA/MODIS and SRTM. Remote Sensing of Environment, 2013, 134, 417-430.
[16] Longbotham, N.; Pacifici, F.; Glenn, T.; Zare, A.; Volpi, M.; Tuia, D.; Christophe, E.; Michel, J.; Inglada, J.; Chanussot, J.; Qian, D. Multi-Modal Change Detection, Application to the Detection of Flooded Areas: Outcome of the 2009–2010 Data Fusion Contest. IEEE Journal of Selected Topics in Applied Earth Observations and Remote Sensing, Volume: 5, Issue: 1,

331 – 342.
[17] Proud, S. R.; Fensholt, R.; Rasmussen, L. V.; Sandholt, I. Rapid response flood detection using the MSG geostationary satellite. International Journal of Applied Earth Observation and Geoinformation, 2011, Volume 13, Number 4, pp 536- 544.Available online http://dx.doi.org/10.1016/j.jag.2011.02.002.
[18] Mandl, D.; Frye, S.; Cappelaere, P.; Handy, M.; Policelli, F.; Katjizeu, M.; Van Langenhove; G.; Saulnier, J. Fr.; Sohlberg, R.; Silva, J. A.; et al. Use of the earth observing one (EO-1) satellite for the Namibia SensorWeb flood early warning pilot. Selected Topics in Applied Earth Observations and Remote Sensing, IEEE Journal of 6, 2013, no. 2 (pp. 298-308.
[19] Chien, S.; Doubleday, J.; Mclaren, D.; Tran, D.; Khunboa, C.; Leelapatra, W.; Plergamon, V.; Tanpipat, V.; Chitradon, R.; Boonya-aroonnet, S.; et al. Combining Space-based and In-situ measurements to track flooding in Thailand, International Geoscience and Remote Sensing Symposium, Vancouver, BC, July 2011.
[20] Chien, S.; Cichy, B.; Davies, A. G.; Tran, D.; Rabideau, G.; Castano, R.; Sherwood, R.; Mandl, D.; Frye, S.; Schulman, S.; et al. An Autonomous Earth-Observing Sensorweb. IEEE Intelligent Systems 2005, Volume 20, Number 3, 16-24.
[21] Chien, S.; Tran, D.; Rabideau, G.; Schaffer, S.; Mandl, D.; Frye, S. Timeline-based Space Operations Scheduling with External Constraints. International Conference on Automated Planning and Scheduling, Toronto, Canada, May 2010.
[22] Ip, F.; Dohm, J. M.; Baker, V. R.; Doggett, T.; Davies, A. G.; Castano, R.; Chien, S.; Cichy, B.; Greeley, R.; Sherwood, R. Development and Testing of the Autonomous Spacecraft Experiment (ASE) floodwater classifiers: Real-time Smart Reconnaissance of Transient Flooding. Remote Sensing of Environment 2005, Volume 101, Number 4, 463-481.Science Direct. Rapid response flood detection using the MSG geostationary satellite. Available online: http://www.sciencedirect.com/science/article/pii/S0303243411000274 (accessed August 2011)..
[23] Schölkopf, B.; Smola, A. J. Learning with kernels. Cambridge, MA: MIT Press 2002.
[24] Mclaren, D.; Doubleday, J.; Chien, S. Using WorldView-2 imagery to track flooding in Thailand in a multi-asset sensorweb. SPIE Defense, Security + Sensing 2012, Baltimore, MD, April 2012.
[25] Pixellearn, NASA Tech Briefs, November 2006.
[26] HAII. Hydrological Model Output. Available online (temporary site): http://tiwrmdev.haii.or.th/swat_output/index.php (accessed December 2012).

EL USO DE SOFT COMPUTING PARA EL MODELADO DEL RAZONAMIENTO

Dra. Daniela López De Luise
(CI2S Labs, IDTI Lab)

Instituto de Comunicaciones Digitales de la Sociedad Científica Argentina

RESUMEN

En la actualidad se emplean términos como Soft Computing, Sistemas Inteligentes, Inteligencia Computacional, entre otros muchos. No es sencillo prepararse para semejante innovación tecnológica formal y normalmente uno se limita a realizar alguna interpretación suficientemente racional sobre su posible significado. En este artículo, se introducirá brevemente una explicación que permitirá al lector apreciar dónde se halla, hacia dónde se dirige este área de la ciencia y tecnología, y cómo podría encararse de manera positiva esta miríada de alternativas que se abre desenfrenadamente a los ojos del profano. Se introducen aquí de manera muy global y simplificada tres teorías originadas en el CI2S Labs y en colaboración con el IDTI Lab. Las mismas son esencialmente una manifestación del poder, variedad y amplitud de estas herramientas sofisticadas y novedosas.
Palabras clave: sistemas inteligentes, onditas lingüísticas morfosintácticas, sistemas armónicos difusos, razonamiento bacteriano

ABSTRACT

Currently, terms like Soft Computing, Intelligent Systems, Computational Intelligence, among many others, are being used. We are not prepared for such formal technological invasion and we limit ourselves to making some quite rational interpretation of them. In this article, I will briefly introduce an explanation that allows the reader to appreciate the status, and where is headed this area of science and technology. Also, how this myriad of alternatives, that wildly opens at profane' sight, could be addressed in a positive way. Three theories originated in the CI2S Labs in collaboration with IDTI Lab are introduced here in a very basic and simplified approach. They are essentially an expression of the power, variety and amplitude of these sophisticated and novel tools.
Keywords: intelligent systems, morphosyntactic linguistic wavelets, fuzzy harmonic systems, bacteria reasoning.

1. INTRODUCCIÓN

Qué se piensa de los sistemas inteligentes

Desde sus inicios, los sistemas inteligentes han pasado por una innumerable cantidad de vaivenes. Los antecedentes no son pocos y dan cuenta de la amplia y compleja relación entre el humano como ente activo que aplica y desarrolla estas herramientas sofisticadas, y el mismo como objeto de su estudio. A pesar de ello, es dable pensar que la relación entre sujeto y objeto de estudio sea cada vez más dinámica y enriquecedora. Como resultado de la evolución han surgido un sinfín de tecnologías, y estrategias que vehiculizan esta relación. Algunas son populares y de amplio uso, como las redes neuronales artificiales. Otras, en cambio, se reservan a minorías que acceden a información altamente especializada y enfocada a fines específicos. En todo caso, es de destacar, que se generan de manera permanente en todo el mundo y con diverso grado de éxito. Pero todas constituyen un avance y, al cabo, una expresión de la necesidad de plasmar en términos de lo que hoy se reconoce como "modelo" del algún problema concreto y, por derivación del mismo, su correspondiente clave de solución.

Tal vez una de las razones de mayor peso sobre el amor-odio desarrollado entre los sistemas inteligentes y las personas del común, sea el lógico desconocimiento de la materia. Cuando se habla de matemáticas, está claro que se trata de una herramienta de descripción numérica que permite introducir en el mundo métrico a ciertos elementos muy abstractos que se manejan en la realidad, tales como sumas, superficies, etc. Incluso se aceptan como elementos de manipulación por parte de otras ciencias como la economía y la física. La química es otra de estas maravillosas herramientas, que aún en su complejidad, se acota en su alcance. Otras ciencias cobran dimensiones menos precisas pero necesarias. Pero cuando se habla de sistemas inteligentes, existe una reactividad cercana al instinto de supervivencia, una inhalación de lo que podría ser un atrevido intento de imitación humana. Y es esta visión la que provocó que los sistemas inteligentes iniciales produzcan el temor humano a ser desplazados por máquinas habilidosas. Dicho temor no sólo impactó en el imaginario popular, generando obras literarias como las del prolífico Isaac Asimov con sus Yo robot (1950) y el hombre bicentenario (1976), sino también películas de cine como IA (2001) del conocido Steven Spielberg. Por supuesto los técnicos y científicos también se vieron afectados y comenzaron esa búsqueda desenfrenada del ser artificial bajo la quimera de un "resolvedor universal de problemas", suficientemente astuto como el humano, pero con la superioridad de las máquinas. El fracaso de esta visión se vio reflejado en el estancamiento y menosprecio de los sistemas inteligentes durante los años 70-80, hasta que un refrescante nuevo concepto salió a la palestra: por fin los sistemas inteligentes se colocaron como una herramienta de características únicas, y no como un competidor del humano. Entonces se dio lugar a las nuevas generaciones de sistemas, estrategias y tecnologías de construcción de soluciones, donde no había tornillos ni acero en vista, sino números, recetas demostrables llamadas algoritmos, estadísticas y otras nuevas recetas automágicas llamadas heurísticos (aquellas recetas que por uso de estadísticas y comprobación empírica son muy útiles en situaciones altamente complejas, pero nadie sabe exactamente por qué funcionan bien).

Paradójicamente, sin embargo, el antiguo temor a las máquinas inteligentes ha ido resurgiendo con toda la fuerza del mito anterior, recrudecido por impactantes muestras de la tecnología. Con robots humanoides que tienen un acentuado aspecto natural, nuevamente el instinto humano se dispara desde su raíz más primitiva aborreciendo un potencial desplazamiento en el espacio laboral, creativo y hasta social. Incluso surgen polémicas sobre si las tres leyes de la robótica planteadas por Asimov sean suficiente escudo protector contra este intruso poderoso de nuestra realidad. Planteos como la moralidad robótica, la ética y responsabilidad criminal se ponen sobre el tapete: ¿Qué tan expuestos están los humanos a estos nuevos seres? Y es bastante curioso porque antaño se consideraba un importante aliado a los autómatas (abuelos de los robots) donde estatuas mecanizadas podían moverse de manera limitada ya antes de la primera obra registrada sobre robots (Autómata, escrito por Herón antes de la primer centuria de la era actual) sólo para representar a dioses o seres especiales, o los robots de Hefestos en la mitología griega que servían para la defensa, al igual que los robots chinos que fueron apostados sobre la gran muralla para espantar a los soldados enemigos, por parecerse físicamente a humanos armados.

También llama la atención tanto temor por los sistemas inteligentes y la robótica por parte de la sociedad mundial, considerando las terribles debacles producidas por el hombre desde que es portador de poder bélico. El foco está demasiado puesto en los seres artificiales, sin considerar que son otra obra más de la propia humanidad, tan destructiva como las bombas nucleares, armas químicas, el hambre, la polución, y otro sinnúmero de amenazas que el hombre ha sabido crear de manera altamente exitosa.

Tal vez, una perspectiva post-mortem de lo que conlleva al desarrollo de sistemas inteligentes muestre, que en realidad el mayor enemigo de la humanidad es la propia humanidad y su falta de evolución a la par de sus creaciones: como un niño que casi inconscientemente llega a crear un juguete peligroso con el cual puede llegar a lastimarse. Pero en ese caso, habría un adulto que protegerá al niño de su propia mano. Entonces, la sociedad mundial deberá hallar un sustituto eficaz en estas instancias en la moral, la empatía y el bien común. Ese será entonces el desafío que se ha de enfrentar.

Sistemas inteligentes: definiciones y más definiciones

Habitualmente las áreas de estudio, al evolucionar introducen de manera más o menos organizada una serie de términos y convenciones para denotar aquellas cosas relevantes que van surgiendo. Lamentablemente la comunidad científica y tecnológica no fue tan organizada como otras áreas. Luego de un caos original, algunas entidades han intentado deshacer dicho caos. Entre ellas el IEEE (Institute of Electrical and Electronic Engineers), sociedad internacional reconocida no sólo por su antigüedad sino también por organizar buena parte de los estándares y nomenclaturas tecnológicas. Entre otras cosas se han definido algunos vocablos por uso y costumbre mayoritario, y otros por determinación ad-hoc. Hoy por hoy, sin embargo, hay colegas que discuten acalorados sobre cómo denotar o explicar ciertos términos. Considero que, la solución propuesta por IEEE es bastante aceptable y salomónica. En general se habla de sistemas inteligentes como un área de conocimiento global que puede abarcar muchas tecnologías. Algunas de ellas son bio-inspiradas pero no todas. En cambio Inteligencia Artificial, se la suele reducir a las técnicas originarias del sector, típica de la década del 60 hasta el surgimiento de los heurísticos, la minería de datos y otras tantas estrategias productivas. En cambio la inteligencia computacional (también llamada Soft Computing en inglés) viene a tomar dominio de los sistemas inteligentes en las últimas décadas. La diferencia a priori es bastante sencilla: estas últimas son típicamente estrategias que requieren poco conocimiento previo del problema a resolver, son muy flexibles y extraen parte de su conocimiento de los propios datos. Por supuesto que la definición técnica es un poco más acabada y a lo mejor un tanto más sutil cuando se hila fino, pero baste con decir que son la lógica evolución de los anteriores, es la dosis adecuada de potencia de cálculo y almacenamiento actual, sumado a la altísima provisión de datos que suele acompañar a los problemas del campo. Es de destacar que en la actualidad, ya los sistemas inteligentes no imitan sólo la inteligencia humana, sino también la biológica, y la increíble astucia de la naturaleza desarrollada en cuestiones que hasta puedan parecer sencillas. Así es que según esta nueva concepción, inteligencia puede ser el comportamiento de una hormiga, la curva de histéresis de los metales, el comportamiento de las neuronas en la retina, etc.

A la par de estas nuevas concepciones, una batería de medidas de calidad y certeza acerca del comportamiento de esos nuevos modelos (o maquetas inteligentes) puede ser aplicada. Lamentablemente no siempre es así y existe una carencia bastante acentuada en este aspecto, que podría poner en peligro la credibilidad de este tipo de tecnologías.

Por eso surge la imperiosa necesidad de que se resguarde con celo dicha credibilidad, fortaleciendo la rigurosidad de estos nuevos sistemas desde dos puntos esenciales:

-Las condiciones de aplicabilidad del sistema

-Las métricas e indicadores de calidad

Mientras los algoritmos se apliquen, se obtendrán resultados. Cual máquina de hacer chorizos los resultados parecerán rigurosos modelos del problema y/o llave invaluable para resolver técnicamente los mismos.

Sin embargo las tablas, números y gráficas, por complejos que se nos aparezcan, no son sinónimo de rigurosidad sino de verborragia matemática insustancial. Para evitar caer en ese lodazal, es menester verificar con rigurosidad si la tecnología inteligente específica que se desea aplicar (reflejada típicamente en algún heurístico o algoritmo) funciona sobre hipótesis de trabajo consistentes a las del problema en cuestión. De no ser así, el resultado será cualquier cosa menos una maqueta del problema o solución perseguido.

Aun suponiendo que ésto se lleve a cabo, queda aún un segundo reto técnico no menor: evaluar la calidad con algún mecanismo y criterio. Allí, el terreno suele ser más pantanoso que el anterior, pues suelen aplicarse mecánicamente ecuaciones y conteos que, o bien no alcanzan a evaluar correctamente la calidad del resultado en el contexto actual, o bien miden más a la muestra operada en la construcción del modelo que a la población representada por dicha muestra.

En todo caso, es obvio que el problema técnico no se limita a la construcción de nuevas estrategias, algoritmos y herramientas automatizadas que nos permitan llegar a resultados más sofisticados. Sin embargo no es tan evidente que dichas evaluaciones se estén llevando tan a la par de los avances en el sector. Por lo que se deriva en una buena cantidad de producción espúrea de trabajos con pretendido viso científico.

2. Onditas lingüísticas morfosintácticas: la matemática increíble del cerebro humano

El cerebro humano es una increíble máquina capaz de un procesamiento asombroso, conservando una plasticidad única. Como ya lo comentara en la introducción, la pretendida meta original de los científicos al pretender imitarla en todo su esplendor, con la tecnología de los 60, provocó un tropiezo considerable del que costó mucho salir.

En la actualidad, se han desarrollado y continúan desarrollando varias modelos que encaran no sólo la resolución de problemas de manera inteligente, sino también modelos de ciertos aspectos del funcionamiento cerebral. Tal vez una actividad que se considera tan natural como lo es el habla, sea de las más complejas de modelar. Interviene una complicada colección de fenómenos y estímulos que se entrelazan y moderan el proceso de emitir una simple oración. Por supuesto que esta complejidad encuentra origen en su propio germen: el razonamiento. A poco que se intente imitar algo del fenómeno, se estará en visión de cuán vasta es la tarea y cuán compleja puede llegar a ser. Prueba de esto son la defectuosidad aceptada de los traductores automáticos y de los sistemas de diálogo automático (también llamados asistentes virtuales, o robots de diálogo).

Pero en dicho mar de factores y efectos entrelazados, los que se dedican afanosamente por ahondar en el razonamiento lingüístico, han logrado algunas victorias con las que es posible vislumbrar que existe un camino largo pero posible por recorrer para poder llegar algún día a un sistema completamente automático de habla.

En lo que hace al estado del arte, varios científicos han desarrollado estrategias que estudian el habla con diferentes enfoques. Muchos de ellos basados en el poder de los ejemplos para aprender a imitar y comprender. Pero a la fecha, hay una barrera no sencilla cuando se trata de la generación de un diálogo amplio y profuso como el que realizaría un humano. Las tendencias actuales parecen querer ahondar en técnicas conocidas como big data (estrategias para grandes cantidades de información sobre cierto tópico), estadísticas o inferencias más o menos sofisticadas. La verdad es que el paso aún no logra ser suficientemente bueno para lograr zanjar el problema de la imitación de un humano a la hora de dialogar de manera mínimamente inteligente y coherente.

En medio de toda esa parafernalia de herramientas, surgen las onditas lingüísticas morfosintácticas (Morphosyntactic Linguistic Wavelets, por sus siglas en inglés, o también MLW). Se trata nuevamente de aprovechar el conocimiento en otras áreas como son las onditas (wavelets) que suelen usarse para describir típicamente el comportamiento de señales (por ejemplo sonidos o imágenes). Su eficiencia y poder radican esencialmente en la capacidad de reducir un comportamiento de la realidad (por caso sea un sonido) en componentes sencillos que, al volver a reunirse de determinada manera logran reconstruir de manera aceptable el fenómeno original (el sonido). Así, esas componentes se pueden emplear con otros fines (por ejemplo depurar el sonido, adaptarlo, simplificarlo, representarlo de manera compacta, etc.).

Manteniendo el mismo espíritu de dichas wavelets, es que se generan las MLW. El desafío mayor consiste en hallar la manera de descomponer sistemáticamente algo que no es matemático, por medios automáticos. Captar la subjetividad y contexto de un mensaje por medio de números, o al menos indicadores que permitan la elaboración de parámetros aceptables de descomposición. Dichos parámetros, una vez reunidos constituyen una cuantización de las características físicas y subjetivas no sólo de las palabras, sino de la frase y levemente del contexto inmediato / mediato de aplicación.

Con semejante descripción es posible, de manera análoga a las wavelets tradicionales, cumplir con otros fines como la búsqueda por contenidos, interpretación de textos y expresiones [2] [3], comprender y medir efectos que tienen ciertas actividades sobre el cerebro (por ejemplo evaluar el impacto del bilingüismo precoz y las alteraciones que produce sobre la capacidad de comprensión profunda del lenguaje) [4], evaluación automática de contenidos en la WEB sin necesidad de indexarlo por fuerza bruta[5] , medir la usabilidad de la Web respecto al uso nativo de la lengua [6], etc. Es interesante destacar que una de las aplicaciones útiles es la derivación de un lenguaje simbólico que represente un texto completo. Simplemente con una corta lista de reglas como la de Fig. 1, se reemplazan porciones de texto por símbolos, incluso se descartan algunas palabra.

Fig. 1. Reglas de conversión texto a símbolos

ID	REGLA	SÍMBOLOS
1	A de B [y | o C[y |o ...]]	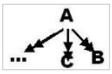
4	A y|e B [XXX]	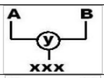
7	A o B [XXX]	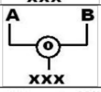
31	**A se B**	**A→B**

La construcción textual, es pasible de ser convertida de manera automática en una gráfica esquemática. La que, al ser evaluada con un grupo de voluntarios, ha probado ser altamente eficaz: La totalidad de los voluntarios fue capaz de reconstruir el texto original de manera exitosa. [7]

El proceso de parametrización se realiza de manera progresiva, a partir elementos de la lengua que son símiles entre sí según criterios morfosintácticos de la palabra, la sentencia y el párrafo. De esa manera se llegan a construcciones como la de la figura 2. Las diferentes palabras, son reemplazadas por sus parámetros de descripción y consideradas como una estructura (Eci). Luego toca que las mismas sean transformadas y comparadas con ellas mismas al ser usadas en otros contextos, y con otras palabras. El resultado son zonas donde se concentran estructuras que representan diferentes conceptos. [8]

Fig. 2. Fenómeno de agrupación por asociación automática de parámetros morfosintácticos

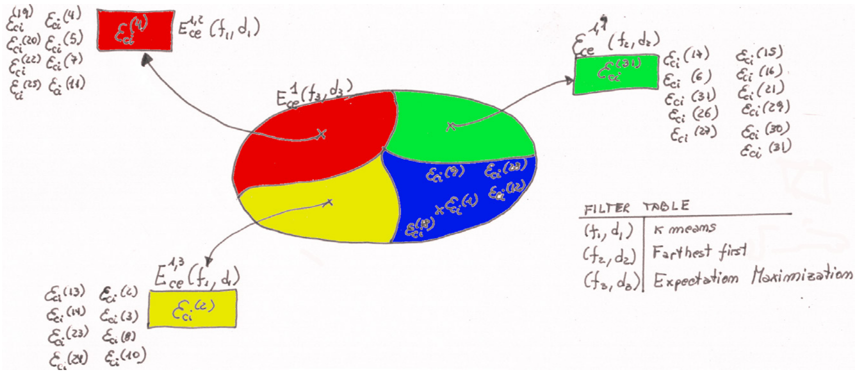

Como es de esperar, el criterio de agrupación deriva en conjuntos que con el tiempo adquieren un tamaño considerable, lo que exige hallar un nuevo criterio de clasificación o discriminación a partir de los elementos dentro de un mismo subconjunto. Así, se debe emplear una sucesión de criterios (en la figura llamado "Filter Table", tabla de filtros).

Esta estructuración progresiva, permite generar en el largo plazo, conjuntos subsumantes (los cuadrados de la figura), que típicamente contendrán aquellas estructuras de mayor abstracción. La hipótesis subyacente en las MLW, es que en este tipo de mecanismos, con escasa intervención artificial del humano para dirigir el proceso, es donde reside la clave para hallar las bases de la síntesis del lenguaje.

Profundizando en este tipo de heurísticos, es que las MLW han permitido evaluar la dinámica de las palabras y los conceptos dentro de las estructuras del lenguaje [9]. Así, se puede visualizar que la selección de las estructuras de las oraciones no son completadas con cualquier tipo de palabras sino que las mismas tienen una peso progresivamente menor según la cantidad de veces que se usa. Así se ve en la figura 3. [9][10]

Fig. 3. Fenómeno de distribución de pesos de palabras según el tipo, conforme se usa en un diálogo

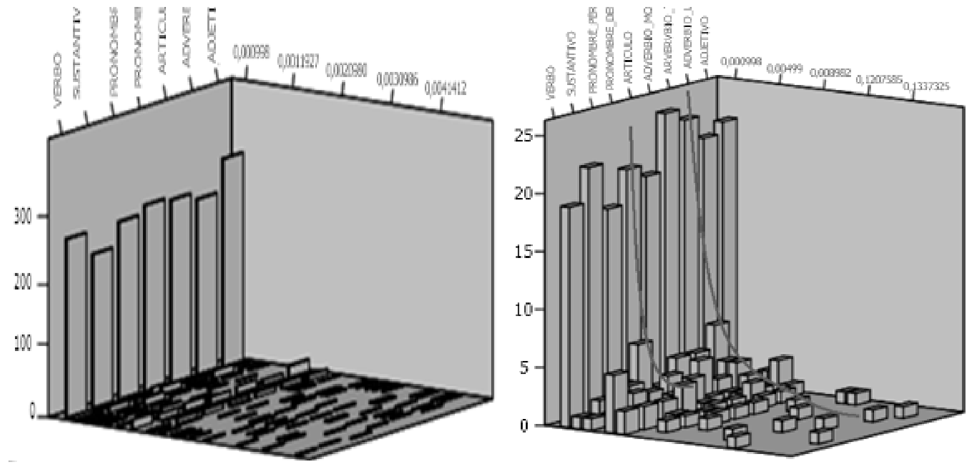

El diagrama de la izquierda muestra barras homogéneamente distribuidas, sin mayor ponderación de ningún tipo por el tipo de palabras, y es que corresponde a textos cuyas oraciones fueron generadas al azar. En cambio las barras de la figura a la derecha muestran un decrecimiento desde un valor inicial dependiente del tipo de palabra. Esta última corresponde al análisis de pesos usando MLW.

Curiosamente, esto coincide con la denominada "Ley de Zipf", que establece un comportamiento similar pero para palabras dentro de un texto para el inglés [12].

Finalmente, otra de las derivaciones interesantes, es la detección de una ley análoga para el comportamiento de los sonidos que producen las palabras empleadas en un diálogo [13] [14], que según los primeros hallazgos seguirían la distribución de un fractal del tipo Dragón. La figura 5 muestra en verde al fractal en cuestión.

Fig. 4. Fenómeno de distribución de palabras en inglés conforme la Ley de Zipf

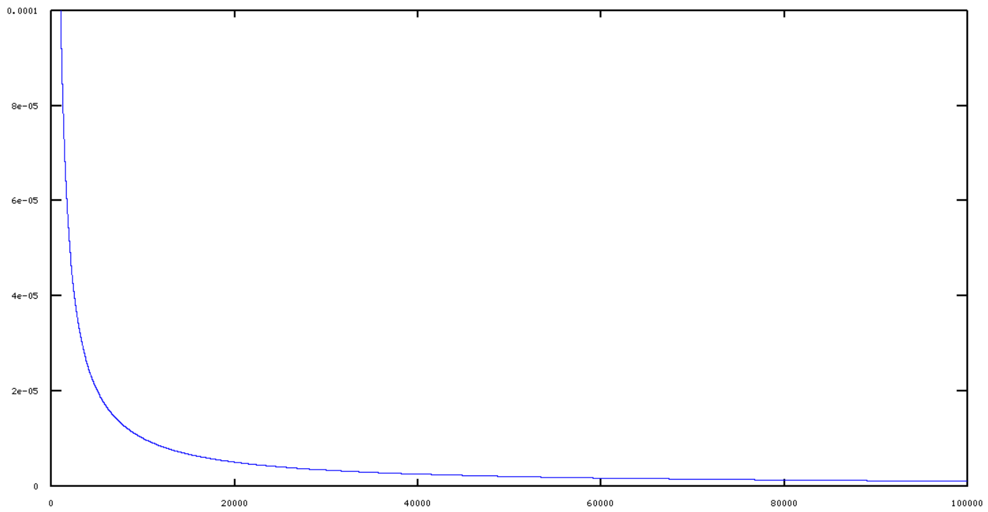

Fig. 5. Fenómeno de distribución de sonidos según el fractal Dragón

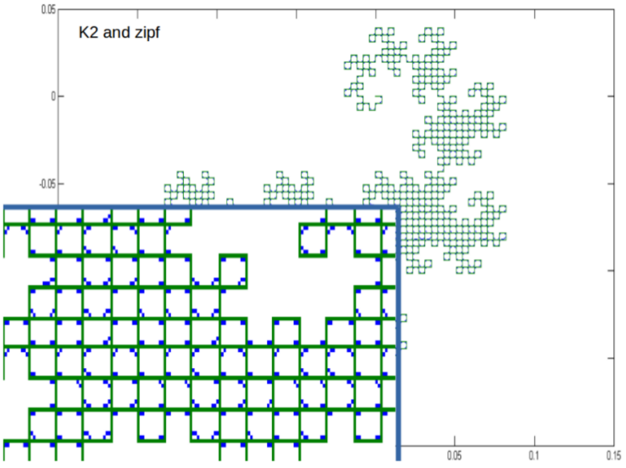

Todos éstos son indicios de que el funcionamiento lingüístico tiene un sustento matemático y estadístico que posibilita la realización de algún tipo de maqueta preliminar. Las palabras, estructuras y sonidos que se producen en el proceso del uso de la lengua constituyen una complicada pero organizada manifestación que sigue leyes precisas. Es menester ahondar en las mismas si es que se desea lograr la generación del habla de manera sintética.

3. Sistemas armónicos difusos: la resonancia de los eventos difusos

Las ondas explican muchos fenómenos interesantes, desde la luz hasta la música pasando por los colores y fenómenos casi mágicos como la difracción. Este poderoso concepto es también considerable como una extraordinaria inteligencia de la naturaleza para lograr ciertos efectos.

Desde el punto de vista ingenieril, es conocido que los sonidos se pueden describir como una suma de ondas específicas que le ofician de componentes, cada una de las cuales a su vez oscila con una velocidad denominada frecuencia. De todas ellas siempre habrá una que es la de menor velocidad o frecuencia, a la que se denomina armónico fundamental. Así, en física y en música un armónico es cualquiera de las ondas componentes, cuya frecuencia sea un múltiplo entero de frecuencia fundamental.

Fundada en la idea de un armónico en música es análogo a un parámetro de un problema a resolver, los sistemas armónicos (Harmonic Systems, HS) centran el modelo de un problema en la descripción de sus parámetros. La colección de dichos parámetros son denominados sellos [15]. Los mismos, al igual que sus análogos de la física, tienen un comportamiento a lo largo del tiempo. Este tipo de modelos tiene una hipótesis de trabajo muy fuerte y es que todos los comportamientos descriptos como sellos son repetitivos con cierta frecuencia. De ahí que se trabaja en cierta analogía con lo ondulatorio.

La ventaja de este enfoque, es que una vez determinado uno o más eventos de interés, el foco de estudio se vuelca meramente a las frecuencias, desplazando del objetivo a la determinación de qué parámetros deberían constituir los sellos.

En la figura 6 se muestra un ejemplo de sello para resolver problemas de acceso en red a recursos especiales, donde cada usuario es identificado por un número. En este problema se supone que se desea detectar y resolver el inconveniente de que el usuario identificado como ID 035 accede al Proceso A (PROC=A), habiendo pasado por el Proceso C y habiendo sido requerido el mismo proceso por el usuario ID 034.

Fig. 6. Sello de problema de acceso

T	PARÁMETRO-1	PARÁMETRO-2
t1=λ_1	PROC=A	USR=034
t2=λ_2	PROC=C	USR=035
t3=λ_3	PROC=A	USR=035

Es importante destacar que en este cuando se pide la ocurrencia del sello, se estudian los lapsos de tiempo transcurridos cuando sucede cada parte del sello. Estos lapsos son denotados en la figura con la letra griega lambda (λ). Una vez detectado que se ha producido el sello completo, se entra en estado de resonancia: el modelo debe activarse. La actividad desempeñada durante la resonancia puede implicar desde disparar alarmas, hasta generar algún tipo de procesamiento. También puede suceder que no exista una actividad especial, pero en todos los casos se procede a actualizar el modelo: los lapsos temporales y las estadísticas sobre la cantidad de veces que el modelo ha resonado son usados para ajustar parámetros adicionales del mismo, entre ellos los rangos de tolerancia para los desvíos en los lapsos entre subeventos (umbral U). La figura 7 muestra las ecuaciones de actualización de U y de los lapsos entre subeventos.

Fig. 7. Actualización durante la resonancia

$$U = U + \eta_u \, (U - P_o(t_1|pattern).P_o(t_2|pattern).P_o(t_3|pattern)$$

$$\lambda_1 = \lambda_1 + \eta \, (t_1 - \lambda_1)$$

$$\lambda_2 = \lambda_2 + \eta \, (t_2 - \lambda_2)$$

$$\lambda_3 = \lambda_3 + \eta \, (t_3 - \lambda_3)$$

Dado que las temporalidades, así como los parámetros pueden no ser precisos, es posible considerar una versión difusa de los mismos, dando lugar a los sistemas armónicos difuso (Fuzzy Harmonic Systems, FHS). Los sellos difusos permiten una mejor representación de los fenómenos que parametrizan el problema cuando éstos caracterizan hechos subjetivos o difíciles de calificar. Aumenta así la potencialidad de los sistemas que aplican esta tecnología.

Entre otras aplicaciones se pueden mencionar la predicción de riesgo de tránsito, para conductor, peatón o ciclista, detección de fallas en tiempo real, detección de fraudes, y en general sistemas de seguridad [16] [17]. En general, se puede decir que son aplicables en sistemas de predicción en tiempo real, donde se requiere el modelado de secuencias complejas de eventos o eventos concomitantes.

Por caso, los FHS usados en la predicción de riesgo de tránsito, han sido comparados con otros métodos basados en sistemas expertos, siendo mucho más potentes y efectivos [18]. Suelen requerir la definición de una serie de parámetros bastante acotados, y han permitido determinar incluso la existencia de variables insospechadas, como por ejemplo la incidencia de la presión atmosférica en la predisposición a accidentes de tránsito [19].

Las figuras 8, 9 y 10 muestran el mapa de definiciones de nivel de riesgo, la interfase de definición de parámetros, y la interfase de registración de un usuario con sus características, parte del prototipo KRONOS [20].

Fig. 8. Mapa de definiciones de riesgo por zonas geográficas

Fig. 9. Interfase de definición de parámetros incluidos en los sellos

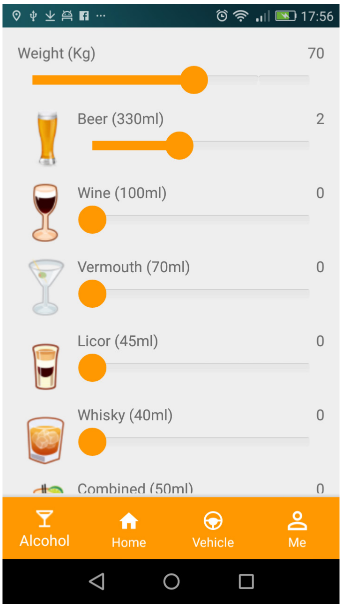

Fig. 10. Interfase de registración de características de usuario (parámetros adicionales)

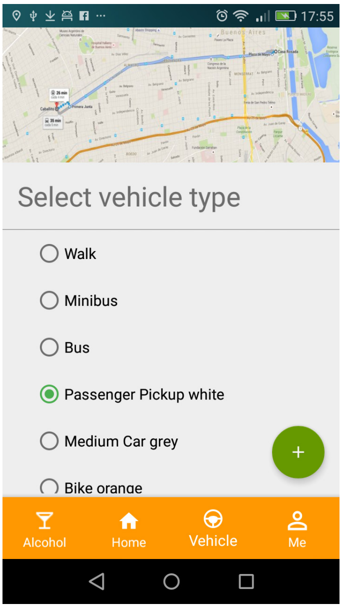

En los resultados logrados con la opción difusa, los sistemas HS han cubierto todos los casos esperables incluso aquellos que quedaban fuera del alcance del sistema experto con la misma información. El precio de esta fortaleza en la capacidad predictiva fue unas fracciones de segundo en la determinación del nivel de riesgo, pero las investigaciones actuales sobre el prototipo permiten adelantar que es posible mejorar el tiempo de respuesta y lograr a la vez resultados interesantes. Como parte del proyecto, el equipo de investigaciones planea generar un repositorio de antecedentes que permita al sistema mejorar su capacidad predictiva al considerar la retroalimentación. A la vez, se estará generando un banco de datos único en su tipo.

4. Razonamiento bacteriano: la adaptabilidad de las bacterias usada como creatividad mecanizada

Entre los modelos inteligentes, están los basados en conciencia. Los mismos fueron planteados por D. Hofstadter [21]. Se basa en la filosofía del sistema que se piensa a sí mismo, y llega a postularlo en su derivación de comprender sobre el mecanismo del pensamiento.

En sus fundamentos se establece cómo surgiría el proceso cognitivo a partir de un conjunto de mecanismos neuronales. El surgimiento de la conciencia, el entendimiento coherente de las cosas se concibe como consecuencia de la acción coordinada de las neuronas del cerebro, de manera análoga y unificada a como lo hacen las colonias de hormigas.

Así esas "hormigas", cuyas actividades son simples y rutinarias, son sinónimo a un concepto denominado "codelet". El total de los codelets existentes se catalogan en un inventario denominado Coderack. Los codelets que se activan interactúan sobre conceptos reforzándolos (promocionándolos a una memoria de largo plazo llamada Slipnet) o dejándolos en el olvido. Por procesos de activación, la acción conjunta y coordinada se realiza en una realidad borrador denominada Workspace, donde la resultante del accionar conjunto de los codelets culmina con un conjunto óptimo de concepts (o nodos) interrelacionados de manera que modelizan adecuadamente el problema en cuestión.

La figura 11 muestra los conceptos más esenciales de los sistemas basados en conciencia.

Fig. 11. Sistema de conciencia (basado en codelets)

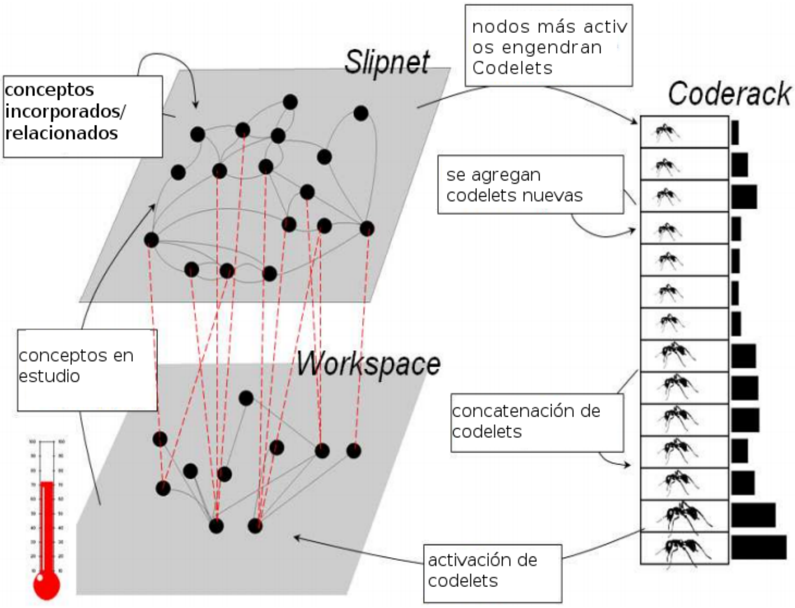

El énfasis más importante de los sistemas basados en conciencia reside en la plasticidad de incorporar conceptos luego de varias tentativas elaboradas en diferentes Workspaces, donde las codelets indagan la posibilidad de que un concepto se pueda asociar a otro y la manera en que dicha asociación se realiza.

En las aplicaciones iniciales de esta teoría, entre cuyos investigadores más relevantes se puede citar a Stan Franklin de la Universidad de Memphis [24], el modelo se construye en base a pesadas rutinas que implementan estos elementos básicos que siguen la teoría inicial de Hofstadter. Sin embargo, para aplicaciones como robótica, dicha estructura se volvía impracticable dado el tiempo de respuesta exigente. Es así que surge una adaptación en un prototipo liviano (COFRAM) que evolucionó progresivamente desde una idea inicial (ALGOC) hasta llegar a una estructura aceptable aún para robots de desplazamiento autónomo. Pero en campo el sistema basado en conciencia presentó problemas de índole práctica en cuanto a que la gran potencialidad del modelo quedaba acotada por la escasa originalidad de los nuevos codelets ingresados al Coderack.

Estos sistemas tienen la fortaleza de la flexibilidad, pero aplicados a ciertos campos carecen de la creatividad adecuada para generar los conceptos abstractos necesarios que organicen esos concepts, y deja al modelo inútil para su uso en ámbitos que exigen resolución rápida, por caso el de la robótica de desplazamiento autónomo. [22]

La adaptación deberá entonces potenciarse con un nuevo concepto que permita a los codelets auto inventarse según lo requieran los concepts del workspace. Es allí donde surge el concepto de razonamiento bacteriano: plasmar la creatividad natural de las bacterias para mejorar la adaptabilidad a nuevas situaciones. En la figura 12 se muestra la cantidad de codelets creados y activados cuando en el entorno no hay obstáculos. La figura 13 muestra la actividad con dos obstáculos.

Lo primero que surge es que la cantidad de codelets activos y su tipo es aproximadamente la misma independientemente de la cantidad de obstáculos (esto es, la complejidad del entorno o problema a resolver). En otras palabras, la conciencia explora usando siempre los mismos elementos de juicio sin explorar otros.

Cuando se incorporan las componentes bacterianas, los codelets se vuelven más variados, y las alternativas de exploración del problema se vuelven más diversos. [23]
Comienzan a surgir conceptos más abstractos y que permiten observar el entorno desde otros puntos de vista más complejos, subsumando detalles del problema que permiten alterar las soluciones originales y lograr mayor creatividad de la solución.

Es interesante observar qué aspectos se han tomado del comportamiento del virus para generar esta flexibilidad bacteriana.

Para poder realizar un procesamiento desde esta teoría, el primer paso es definir un virus, lo que se realiza de manera algorítmica. Entonces deben asociarse las características fundamentales del problema actual a resolver, con ciertas variables que las representan. El conjunto de dichas variables actuarán como estado del modelo, y su evolución será desde un estado actual (inicial) hacia otro final. Estos estados varían acorde a los procesos asociados al virus.

Fig. 12. Actividad de los Codelets cuando no hay obstáculos

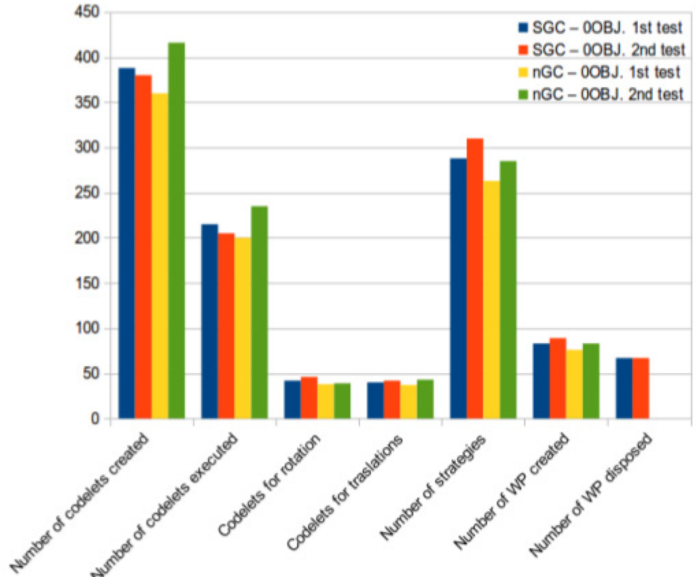

Fig. 13. Actividad de los Codelets cuando hay 2 obstáculos

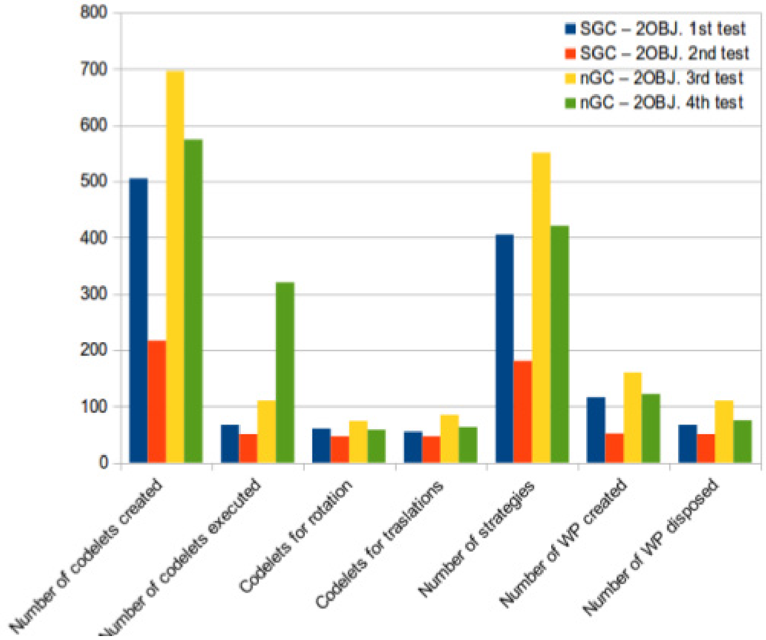

El siguiente paso es definir al virus per se. Eso se logra caracterizando las distintas acciones posibles del mismo sobre el organismo como secuencias de los siguientes elementos: estado inicial, proceso, entradas, salidas. Las definiciones en cuestión serán por medio de funciones auto adaptativas, esto es, funciones que pueden cambiar su funcionamiento radicalmente de acuerdo a la combinación actual de entradas y salidas. Los elementos constitutivos de un virus típico se observan simbolizados en la figura 14.

Fig. 14. Determinación de un VIRUS

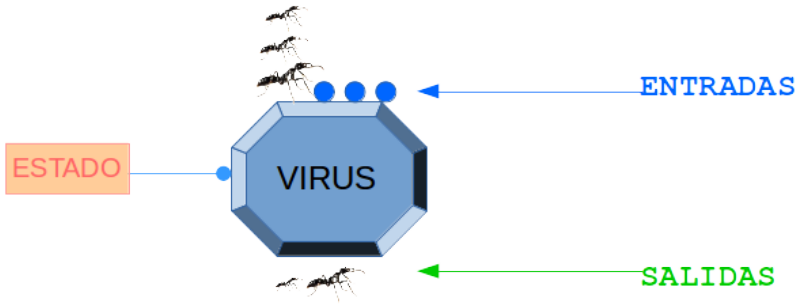

Como se puede apreciar, las entradas pueden ser codelets o conceptos, pero las salidas son típicamente codelets, puesto que el comportamiento bacteriano se está aplicando a la generación de codelets más creativos para el Coderack.

En este contexto se considera como "organismo" a infectar al modelo actual, representado por un estado y uno o más habilidades de acción (denominados procesos). El organismo se infecta inicialmente y luego se desarrolla una colonia, con características propias determinadas probabilísticamente por el conjunto de alteraciones posibles a los procesos actuales que caracterizan al organismo.

El proceso de infección puede ser selectivo o masivo, y al final del proceso se evalúa el estado del individuo (la viabilidad del nuevo "organismo" como ente resolvedor del problema en cuestión).

En la figura 15 se observan el organismo, y el efecto de la infección.

Fig. 15. Infección selectiva de un VIRUS

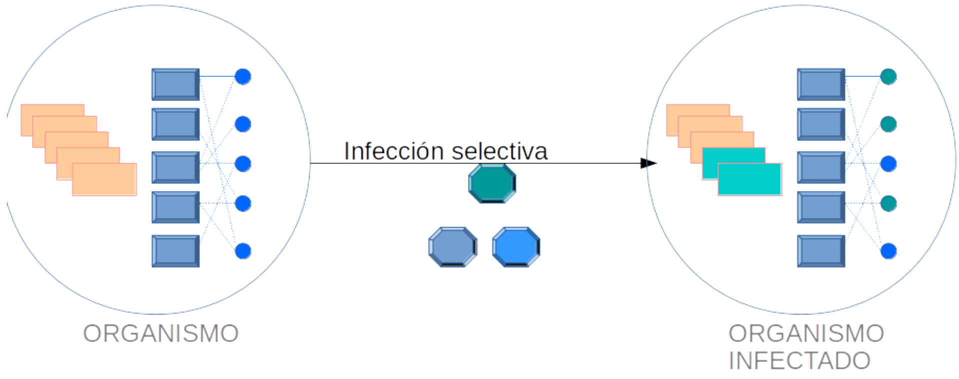

Se observa en la figura al estado actual (rectángulos), funciones o habilidades normales del modelo (rectángulos) y codelets (círculos), que por infección selectiva de uno de los virus (polígono) termina en un modelo con un estado diferente, y codelets alteradas.

El proceso deriva en un modelo nuevo no sólo con un estado diferente, sino también con capacidades diferentes.

5. Conclusiones

Las tecnologías emergentes en el área de los sistemas inteligentes permiten vislumbrar un futuro prometedor en varias áreas, y es de esperar que surjan nuevas áreas en la medida que su evolución muestre las potencialidades que hoy en día sólo se perciben remotamente. Es deber de la comunidad en su totalidad guiar este proceso de manera responsables de modo que la evolución de las mismas signifique una evolución y la tan ansiada respuesta a diversas problemáticas que hoy en día son de compleja solución. La responsabilidad, como siempre, se halla no en las herramientas que se engendren con el poderosísimo cerebro humano, sino en el uso que se dé a las mismas.

Referencias

[1] A Morphosyntactical Complementary Structure for Searching and Browsing". D. López De Luise. Proc. of International Conference on Systems, Computing Sciences and Software Engineering (SCSS 2005). Springer 2008, ISBN 1-4020-5262-6 págs. 283 – 290.
[2] Del procesamiento de la lengua al razonamiento lingüístico: Morphosyntactic Linguistic Wavelets. D. López De Luise.The IEEE Latin America and the Caribbean Magazine. NoticI-EEEro # 84, pp 38 - 42. vol. 24, n. 4. August 2013. ISSN 2151-8354.2013
[3] Ambiguity and Contradiction from a Morpho-Syntactic Prototype Perspective. D. López De Luise. International Joint Conferences on Computer, Information, and Systems Sciences, and Engineering. CISSE 2007. Springer Verlag, ISBN 978-1-4020-8734-9. pags. 154 – 158.
[4] MLW and bilingualism (bilingüismo y MLW). D. López De Luise, D. Hisgen. Advanced Research and Trends in New Technologies, Software, Human-Computer Interaction, and Communicability. Francisco Vicente Cipolla-Ficarra IGI Global, Hershey – USA. Fecha: agosto de 2013. DOI: 10.4018/978-1-4666-4490-8, ISBN13: 9781466644908. 2013.
[5] Webcrawling clustering en espacio multidimensional basado en distancia y su aplicación a Opinion Mining. M. Daniela López De Luise, et al. Ciencia y Tecnología, 12, 2012, pp. 7-25. ISSN 1850-0870
[6] Usabilidad de la Web, lingüística y morfosintaxis: Fundamentos de computación lingüística para browsing y wavelets morfosintácticas (Edición en castellano)". Ed.Acad. Española. ISBN-10: 3659034061, ISBN-13: 978-3659034060. 2013
[7] Language Modeling with Morphosyntactic Linguistic Wavelets. López De Luise, D. Hisgen. "Automatic content extraction on the web with intelligent algorithms". CIDM. 2013.
[8] Automatically Modeling Linguistic Categories in Spanish.M. D. López De Luise, D. Hisgen, M. Soffer. International Joint Conferences on Computer, Information, and Systems Sciences, and Engineering (CISSE 09). December 4 - 12, 2009. Sponsored by the University of Bridgeport Technically co-sponsored by the IEEE Computer Society, Communications Society and Education Society (Connecticut Section).
[9] Dialog Structure Automatic Modeling. López De Luise et al. En Proc. LNAI del 9° conferencia internacional mejucana en Artificial Intelligence (MICAI 2010). Noviembre 8-13, 2010, Pachuca, Mexico. México.
[10] Morphosyntactic Linguistic Wavelets for Knowledge Management. Libro "Intelligent Systems", ISBN 979-953-307-593-7. InTech OPEN BOOK. 2011.

[11] Sound Model for Dialogue Profiling. D. López De Luise, R. Azor. International Journal of Advanced Intelligence Paradigms archive. Volume 9 Issue 5-6, January 2017 . Pages 623-640. 2017.
[12] Zipf's word frequency law in natural language: A critical review and future directions. Piantadosi, S. T. Psychonomic Bulletin and Review. 2015.
[13] Métricas Epistemológicas para modelos basados en fractales lingüísticos de PLN. D. López De Luise, M. E. Márquez, C.Párraga. IEEE Biennial Congress of Argentina. Pages: 1 - 7, DOI: 10.1109ARGENCON.2016.7585257 Electronic ISBN: 978-1-4673-9765-0, CD-ROM ISBN: 978-1-4673-9764-3, ISBN: 978-1-4673-9766-7. 2016
[14] Metrics for Epistemology in NLP Linguistic Fractal Models. D. López De Luise, M. E. Marquez, C.Párraga, I. Cayla, R. Azor, V. Ocanto, O. Del, J. López Quel, J. Morelli, M. Agüero, R. Aparicio. 7th International Conference on Information Technologies and Information Society. 2016
[15] Harmonics Systems for Time Mining. D. López De Luise. International Journal of Modern Engineering Research (IJMER). 2014. Este paper ha sido galardonado por el comité editorial por su calidad y relevancia.
[16] Traffic & Pedestrian risk inference using Harmonic Systems. I. Acuña, E. García, D. López De Luise, C. Paredes, A. Celayeta, M. Sandillú, W. Bel KRONOS.2014 Sofa
[17] Predicción de Riesgo basado en tiempo y patrones GPS. D. López de Luise, Walter Bel, Diego Mansilla, Alberto Lobatos, Lucía Blanc. ARGENCON 2016.IEEE Conference Publications. PP. 1/7, DOI: 10.1109/ARGENCON.2016.7585257, e-ISBN: 978-1-4673-9765-0, CD-ROM ISBN: 978-1-4673-9764-3, (PoD) ISBN: 978-1-4673-9766-7. 2016
[18] Parametric Prediction Model using Expert System and Fuzzy Harmonic System. W. Bel , D. López De Luise, A. Asmis, D. Mansilla. Adv. in Intelligent Systems and Computing. ISSN 2194-5357.Springer Verlag. 2016.
[19] Cálculo de Riesgo en tráfico y peatón usando Sistemas Armónicos. D. López De Luise, W. Bel. ISBN del libro (978-3-639-53739-0). EAE. 2017.
[20] Fuzzy Logic in Predictive Harmonic Systems. W. Bel, D. López De Luise, F. Costantini, I. Antoff, L. Alvarez, L. Fravega. SOFA2018. Advances in Intelligent Systems and Computing. (ISSN: 2194-5357). 2018
[21] Gödel, Escher, Bach: An Eternal Golden Braid. Douglas Hofstadter. ISBN 978-0-465-02656-2. 1979
[22] A conscious model for autonomous robotics: Statistical evaluation. D. López De Luise, L. Rancez, N. Biedma, B. de Elía. International Journal of Advanced Intelligence Paradigms (IJAIP) - Inderscience Publishers. 2014.
[23] Evolution of Consciousness Systems with Bacteria. D. López De Luise, L. Rancez, M. Maciel, B. De Elía, J. Menditto. Intelligent Data Analysis for Biomedical Applications: Challenges and Solutions. 2018
[24] A LIDA cognitive model tutorial. S. Franklin et al. Biologically Inspired Cognitive Architectures. 16: 105–130. doi:10.1016/j.bica.2016.04.003.

EX DIRECTORES DE LOS ANALES DE LA SOCIEDAD CIENTÍFICA ARGENTINA (*)

Ing. Pedro Pico
Ing. Luis A. Huergo
Dr. Carlos Berg
Dr. Estanislao S. Zeballos
Ing. Eduardo Aguirre
Ing. Carlos Bunge
Dr. Angel Gallardo
Dr. Félix F. Outes
Dr. Horacio Damianovich
Ing. Julio R. Castiñeiras
Ing. Emilio Rebuelto
Ing. José S. Gandolfo
C. de Nav. Emilio L. Díaz
Dr. Pedro Cattáneo
Ing. Guillermo White
Dr. Valentín Balbín
Ing. Luis A. Viglione
Dr. Carlos María Morales
Ing. Jorge Duclout
Ing. Miguel Iturbe
Ing. Domingo Nocetti
Ing. Santiago Barabino
Dr. Eduardo Carette
Dr. Claro D. Dassen
Ing. Alberto Urcelay
Dr. Reinaldo Vanossi
Dr. Andrés O. M. Stoppani
Dr. Eduardo A. Castro
Dr. Alfredo Kohn Loncarica

(*) Desde 1876 a 1902: Presidente de la Comisión Redactora.

PRESIDENTES HONORARIOS DE LA SOCIEDAD CIENTÍFICA ARGENTINA

1.- Prof. Dr. Andrés O. STOPPANI † (1915 - 2003)

2.- Dr. Carlos Pedro BLAQUIER (1927)

Director Administrativo: Lic. J. M. Lentino

Secretarios Administrativos: Sra. Natalia Lentino y Sr. Pablo A. Riquelme

INSTITUTOS DE LA SCA

Coordinador: Dr. N. Sarubinsky Grafin.

Directores:

- **De Historia de las Ciencias:** Prof. N. I. Sánchez.
- **De Energías Renovables:** Prof. H. Bosch – Dr. R. Vaccaro.
- **De Investigaciones Junguianas:** Prof. Dr. A. Las Heras.
- **De Tecnología de los Alimentos:** Lic. A. Bosch.
- **De Investigación e Innovación Productiva:** Ing. Prof. J. J. Sallaber.
- **Sánchez Labrador:** Prof. Dr. J. Sellés Martínez.
- **De Comunicaciones Digitales:** Ing. E. Draier.
- **De Investigación del HACRE:** Prof. R. P. Rothlin.
- **Del Boletín electrónico:** Lic. E. Laplagne.
- **De Ciencia para la Innovación:** Dr. Ricardo A. López.

INSTRUCCIONES PARA LOS AUTORES

Las siguientes *Instrucciones para los autores* constituyen el reglamento de publicaciones de los ANALES DE LA SOCIEDAD CIENTIFÍCA ARGENTINA.

1) Generales

Los ANALES DE LA SOCIEDAD CIENTÍFCA ARGENTINA constituyen una revista multidisciplinaria, fundada en 1876, que considera para su publicación trabajos de cualquier área de la ciencia.

Los originales deben ser enviados al director, a Av. Santa Fe 1145, Buenos Aires, CP.:1059, República Argentina, en tres copias en papel, a dos espacios, tamaño carta, acompañados de su correspondiente CD. Los CD deberán estar rotulados con el nombre del autor o del primer autor si son varios haciendo constar el sistema computacional usado para grabar el mismo, el tipo y versión del procesador utilizado y nombres de los archivos.

Los autores serán notificados de inmediato de la recepción de sus originales. Dicha notificación no implica la aceptación del trabajo. Los originales son enviados a uno o más 'arbitros, quienes asesoran al director y a la comisión de redacción acerca de la aceptación, rechazo o sugerencia de modificaciones. La decisión final respecto a la publicación o no del trabajo es solamente responsabilidad del director.

Los originales remitidos para su publicación en los ANALES deben ser inéditos y no hallarse en análisis para su publicación en otra revista o cualquier otro medio editorial.

Todo trabajo aceptado en los ANALES no podrá ser publicado en otro medio gráfico sin previo consentimiento de la dirección.

Los ANALES se reservan el dercho de rechazar sin más trámite a aquellos originales que no se ajusten a las normas expuestas en la presente guia de *Instrucciones para los autores.*

Los ANALES constan de las siguientes secciones:

- -artículos de investigación
- -notas breves de investigación
- -articulos de revisión y/o actualización
- -editoriales
- -recensiones
- -cartas a la dirección
- -informaciones del quehacer de la SOCIEDAD CIENTIFICA ARGENTINA
- -informaciones científicas y acádemicas de interés general

Los autores, al remitir sus trabajos, deberán hacer constar la sección, a la que según su juicio, corresponden sus aportes y consignar claramente la dirección postal, teléfono, fax y dirección electrónica (si la tuviere) a la cual se remitirá toda información corceniente al original.

2) Originales

Los ANALES DE LA SOCIEDAD CIENTIFICA ARGENTINA publicarán trabajos escritos en los idiomas: español, francés, inglés y portugués.

Los originales deberán respetar la siguiente estructura:

1ª pagina:

- -Título del trabajo: no mayor de veinticinco (25) palabras
- -Nómina de los autores, institución o instituciones a la que pertenecen cada uno de ellos.
- -Institución en la que se llevó a cabo el trabajo en el caso que difiera de la institución de pertenencia.
- -Domicilio postal y electrónico (si lo tuviere)

2ª página:

- -Resumen en idioma español de no más de 400 palabras, con su correspondiente traducción al inglés. La traducción al inglés deberá incluir el título del trabajo cuando éste haya sido escrito en español y viceversa, si el trabajo se halla escrito en inglés el resumen en español deberá incluir la traducción del título.
- -La inclusión de resumenes en francés y portugués es facultativa de los autores.
- -Palabras claves para el registro bibliogáfico e inserción en bases de datos, en español e inglés.

En las páginas siguientes se incluirán las secciones Introducción, Materiales y Métodos, Resultados, Discusión, Agradecimientos y Referencias. A continuación se agregarán las tablas con sus títulos, leyendas de las figuras y gráficos y finalmente las figuras y gráficos preparados como se indica más abajo.

El tipeado del manuscrito deberá hacerse a doble espacio en papel tamaño carta (aprox. 21 cm x 29cm), dejando 3 cm de márgenes izquierdo, superior e inferior, debiéndose numerar secuencialmente todas las páginas.

No se aceptará la inserción de notas de pie de página. Cuando ello sea necesario, se deberá incluir tales notas en el mismo texto.

Se recomienda emplear el Sistema Métrico Decimal de medidas y las abreviaturas universales estándar.

Solo se permitirá el empleo del Sistema Internacional de Unidades para las medidas.

Como regla general no se deberá repetir la misma información en tablas, figuras y texto. Salvo en casos especiales que justifiquen alguna excepción se aceptará presentar esencialmente la misma la información en dos formas simultáneas.

Cada sección se numerará consecutivamente, recomendándose no emplear subsecciones.

3) Tablas

Las tablas deben prepararse en hojas aparte y a doble espacio. Las mismas incluirán un título suficientemente aclaratorio de su contenido y se indicarán en el texto su ubicación, señalándolo con un lápiz sobre el margen izquierdo.

Cada tabla se numerará consecutivamente con números arábigos. Solo se deberá incluir en las tablas información significativa, debiéndose evitar todo dato accesorio y/o que pueda ser mejor informado en el mismo texto del trabajo.

Cada tabla se tipeará en hoja separada.

Los títulos de las filas y las columnas deben ser lo suficientemente explícitos y consistentes, pero al mismo tiempo se recomienda concisión en su preparación.

4) Ilustraciones

Las ilustraciones (gráficos y fotografías) deberán ser de suficiente calidad tal que permitan una adecuada reproducción debiéndose tener en cuenta que la reproducción directa de los mismos conlleva una relación entre 1:2 y 1:3. Todas las ilustraciones se numerarán consecutivamente y en el reverso de las mismas se indicarán con lápiz blando el nombre de los autores, el número de la misma y cuando corresponda la orientación para su pertinente impresión.

Los títulos de las ilustraciones se tipearán en hoja aparte, debiéndose denotar el posicionado de las mismas en el texto por medio de una indicación con lápiz en el margen izquierdo.

Las dimensiones de las ilustraciones no deberán exceder las de las hojas del manuscrito y no se deberán doblar.

Los gráficos se dibujarán con tinta china sobre papel vegetal de buena calidad y por los mismos medios se incluirán los símbolos, letras y números correspondientes. No se deberá tipear símbolo, letra o número alguno en los gráficos y fotografías.

Enviar un original y dos copias de cada ilustración. Las fotografias solo se podrán enviar en blanco y negro, ya que que no es posible imprimir fotografias en otros colores.

Cada ilustración se presentará en hoja separada.

5) Referencias

Los ANALES adoptan el sistema de referencias por orden, el cual consiste en citar los trabajos en el orden que aparecen por medio de número cardinal correspondiente. Los libros se indicarán en la lista de referencias citando el/los autor/es, título, edición. editorial, ciudad, año y página inicial. Para indicar capítulo de libro se añadirá a lo anterior el título del mismo y el nombre del editor.

El listado de referencias se tipeará en hoja separada y a doble espacio. Se recomienda especialmente a los autores emplear las abreviaturas estándar sugeridas por las propias fuentes.

Solo se admitirán citas de publicaciones válidas y asequibles a los lectores por los medios normales debiéndose evitar recurrir a informes personales, tesis, monografías, trabjos en prensa, etc., de circulación restringida.

Lo que sigue son algunos ejemplos de citas bibliográficas en la lista de referencia:

Publicación periódica: A. M. Sierra y F. S. Gonzalez, J. Chem. Phys. 63 (1977) 512.

Libro: R. A.. Day, How to write and publish a Scientific paper, Second Edition, ISI Press, Philadelphia, 1983, p 35.

Capítulo del libro: Z. Kaszbab, Family Tenebrionodae en W. Wittmer and Buttiper (Eds.) Famma of Saudi Arabia, Ciba-Geigy, Basel, 1981, p3-15.

Conferencia o Simposio: A. Ernest, Energy conservation measures in Kuwait buildings. Proccedings of the First Symposium on Thermal Insulation in the Gulf States, Kuwait Institute for Scientific Research, Kuwait, 1975, p 151.

Se recomienda revisar cuidadosamente las citas en el texto y la lista de referencias a los efectos de evitar inconsistencias y/u omisiones.

Pruebas: todo artículo deberá ser revisado en la forma de prueba de galera por el autor indicado en la carta de presentación del trabajo, la cual se devolverá debidamente corregida a las 72 horas de recibida a la redacción de los ANALES. No se admitrá en forma alguna alteración sustancial del texto y en caso imprescindible se procederá a la inclusión al final del trabajo de lo que correspondiera bajo el título de “ Nota agregada en la prueba”.

ANALES DE LA SOCIEDAD CIENTÍFICA ARGENTINA

www.revistaanalessca.wordpress.com

Órgano de la Sociedad Científica Argentina.

Revista fundada el 14 de diciembre de 1875, cuyo primer número apareció el 14 de enero de 1876.

Se viene editando continuadamente desde esta fecha.

Impreso por:

Systems IMPRESS

stms@fibertel.com.ar

Buenos Aires, Mayo 2019

ISSN 0037-8437

ANALES
DE LA
SOCIEDAD CIENTIFICA
ARGENTINA

AÑO 2019 - VOLUMEN 265 - Nº 1

SUMARIO

Pág.

A.Alonso, A.B.Pomilio, S.R.Rodríguez, S.M.Battista, K.Mouchián, A.Vitale - "FUNGAL HYPERSENSITIVITY IN NASAL PATHOLOGIES". 5

Steve Chien, David Mclaren, Joshua Doubleday, Daniel Tran - USING HIGH-RESOLUTION, TASKABLE REMOTE SENSING IMAGERY TO SUPPORT A SENSORWEB FOR THAILAND FLOOD MONITORING 17

Dra. Daniela López De Luise - EL USO DE SOFT COMPUTING PARA EL MODELADODEL RAZONAMIENTO 39